scientific reports

Check for updates

OPEN

Membrane-targeted immunogenic compositions using exosome mimetic approach for vaccine development against SARS-CoV-2 and other pathogens

Fikret Sahin[1,4]✉, Buse Turegun Atasoy[1], Suleyman Yalcin[2] & Verda Ceylan Bitirim[3]

The COVID-19 pandemic has underscored the urgent need for a vaccine strategy that is safe, effective, rapid, cost-efficient, and scalable for large-scale deployment during widespread infectious outbreaks. Here, we present a new vaccination strategy that meets these critical requirements. The SARS-CoV-2 S protein consists of the S1 and S2 subunits. The S2 subunit acts as the viral cell membrane fusion protein, and mutations in its C-terminal region facilitate the transport of the entire S protein to the cell membrane. When we expressed the SARS-CoV-2 S protein with a deletion of 21 amino acids from its C-terminal region in various cell types, we observed a dense presence of the protein in the cell membrane, as determined by IHC, dot blot, and ELISA. In the cell membrane-SARS-CoV-2 S protein complex, the cell membrane functions as an exosome mimic, carrying protein antigens (S protein) in their most natural form, as no further protocols are used to attach antigens to the membrane. We demonstrate that using the membrane-S protein component as a vaccine yields a more robust and protective immune response, with enhanced safety compared to mRNA-based or inactivated virus-based vaccines against SARS-CoV-2. Additionally, we show that fusing the transmembrane domain of the Vesicular Stomatitis Virus (VSV) G protein with the SARS-CoV-2 S1 protein effectively transports the S1 protein to the cell membrane, similar to SARS-CoV-2 S Δ21. We propose that designing the S2 subunit of the SARS-CoV-2 S protein, or its analogues such as the VSV-G protein, as carriers for fusing bacterial, viral, or tumor proteins with antigenic properties—and transporting them to the cell membrane—could result in a comprehensive vaccination protocol applicable to all bacteria, viruses, and even tumors.

Keywords Exosome-mimetic vaccine model, Transmembrane protein, SARS-CoV-2

The COVID-19 pandemic continues to pose a considerable threat worldwide. Most importantly, the pandemic necessitates a safe, effective, fast, and inexpensive vaccine that can be prepared in bulk for emergencies. Exosomes are extracellular vesicles released from cells when an intermediate endocytic compartment fuses with the plasma membrane. Their structure, similar to the cell membrane, consists primarily of proteins and lipids[1,2]. As natural nanocarriers, exosomes are secreted by various cells, making them suitable for diverse applications, including protein antigen and drug delivery. The stable lipid bilayer of exosomes protects their cargo from the immune system and circulating hydrolases. However, their therapeutic applications are limited by insufficient purification yields; large sample volumes are needed to obtain enough exosomes for therapeutic use[1,2].

To address this issue, exosome mimetics—nanoparticles coated with cell membranes that mimic exosomes—have emerged as promising drug delivery platforms. Recently, different membrane-coated nanoparticles have been developed using membrane isolates from various cells, such as cancer and macrophage cell membranes[3,4].

The SARS-CoV-2 S protein is composed of two subunits, S1 and S2, with a total length of 1,273 amino acids. It includes a signal peptide (amino acids 1–13) at the N-terminus, the S1 subunit (residues 14–685),

[1]Department of Medical Microbiology, University of Ankara, Ankara 06100, Turkey. [2]Microbiology Reference Laboratory, General Directorate of Public Health, Ankara 06800, Turkey. [3]Stem Cell Institution, University of Ankara, Ankara 06520, Turkey. [4]Faculty of Medicine, Department of Medical Microbiology, Ankara University, Morphology Building, Sihhiye, Ankara 06100, Turkey. ✉email: fsahin29@hotmail.com

and the S2 subunit (residues 686–1273). Within the S1 subunit, there are the N-terminal domain (residues 14–305) and the receptor-binding domain (residues 319–541). The S2 subunit contains the fusion peptide (FP) (residues 788–806), heptapeptide repeat sequences HR1 (residues 912–984) and HR2 (residues 1163–1213), the transmembrane (TM) domain (residues 1213–1237), and the cytoplasmic domain (residues 1237–1273)[5].

This invention is based on the insightful research into the intracellular targeting signal region of the spike protein of the Coronavirus, as thoroughly described by various studies that have significantly contributed to our understanding of the virus's interactions within cells[6–8]. According to their findings, Coronavirus budding at the endoplasmic reticulum-Golgi intermediate compartment (ERGIC) requires the accumulation of viral envelope proteins at this point in the secretory pathway. They demonstrated that the spike (S) protein from the group 3 coronavirus, infectious bronchitis virus, contains a canonical dilysine endoplasmic reticulum retrieval signal (-KKXX-COOH) in its cytoplasmic tail. This signal can retain a chimeric reporter protein in the ERGIC, and when mutated, it allows the transport of the full-length S protein as well as the chimera to the plasma membrane[7].

In relation to the findings described by Lontok et al.[7], Boson et al.[8] demonstrated that the envelope (E) and membrane (M) proteins regulate the intracellular trafficking and processing of the spike (S) protein. Their data reveal that the S protein is relocalized to the ER-Golgi intermediate compartment (ERGIC) or Golgi apparatus upon coexpression of E or M, similar to observations in SARS-CoV-2-infected cells, which prevents syncytia formation. They also showed that a C-terminal retrieval motif in the cytoplasmic tail of S is necessary for its retention in the ERGIC mediated by M, whereas E induces S retention by modulating the cell's secretory pathway. Moreover, they demonstrated that the S protein, when deleted in the C-terminal region, is transported to the plasma membrane and predominantly located there, leading to syncytia formation.

They concluded that the C-terminal moiety of the SARS-CoV2-S cytoplasmic tail is essential for the retention of the S protein in the ERGIC compartment.

Therefore, we hypothesize that the ectopic expression of the SARS-CoV2-S protein with a 21-amino-acid deletion from the C-terminal (SARS-CoV-2-S Δ21) in the cell, without M expression, will result in its dense localization at the cytoplasmic membrane rather than remaining in the ERGIC. Additionally, the absence of the E protein is expected to enhance the secretion of SARS-CoV2-S towards the cell membrane and prevent its retention in the ERGIC, thereby allowing the full protein, including both S1 and S2 subunits, to be transported to the cell membrane.

This modification allows us to obtain the natural structure of the SARS-CoV-2 S protein on the cell membrane, forming a cell membrane-S protein complex. The cell membrane thus acts as a natural carrier for the S protein, allowing it to integrate onto the membrane without the need for in vitro addition, unlike the process of adding antigens to exosomes. This results in a more natural mimicry of exosome-nanoparticle complexes.

To test this hypothesis, we prepared cells expressing SARS-CoV-2-S Δ21 and subsequently obtained a cell membrane-S protein complex, which we used as a novel vaccination strategy. We investigated its immune response and compared it to that of mRNA-based and inactivated virus-based vaccines, assessing the potential for uncontrolled cytokine release associated with this vaccination.

In summary, we present a novel vaccination strategy that leverages the transmembrane capability of the S protein to deliver the antigen to the cell membrane. Vaccine safety is a critical concern, as some vaccines can trigger an uncontrolled cytokine storm in certain individuals, potentially leading to acute respiratory distress syndrome (ARDS)[9]. Our study demonstrates that the SARS-CoV-2 S protein-cell membrane composition does not induce uncontrolled cytokine release in vivo in mice. Furthermore, this method allows for the rapid and cost-effective production of large quantities of the composition in its native form, solely through cell proliferation, indicating that it is both effective and safe.

Additionally, our study demonstrates that protein regions with transmembrane (TM) functionality, such as the TM region from the Vesicular stomatitis virus G protein (VSV-G), can be used to replace the TM region of the SARS-CoV-2 S protein. This substitution effectively facilitates the transport of the S protein to the cell membrane, indicating that various TM regions can serve as versatile carriers for antigen presentation.

Importantly, this method can be applied not only for COVID-19 vaccination but also for vaccination against other microbial agents, including viruses and bacteria, as well as for cancer vaccination-treatment. This is achieved by combining any protein or epitope with antigenic properties, including tumor-associated antigens, with the S2 Δ21 subunit, the VSV-G TM domain, or any sequence with transmembrane (TM) function. Therefore, these TM-functioning components serve as carriers for the antigen to the cell membrane, enabling the antigen-membrane composition to be used as a versatile vaccination platform.

Results

SARS-CoV-2 S Δ21 protein overexpression localizes Spike protein to the cell membrane

We examined the expression of the SARS-CoV-2 S protein in cells expressing either the SARS-CoV-2-S Δ21 variant or the wild type (wt) using the pRetroX vector system, a tetracycline-inducible retroviral mammalian expression system controlled by doxycycline (Dox) in the culture medium. The Retro-X Tet-On Advanced Inducible Expression System requires two retroviral constructs: the tetracycline-dependent rtTA transactivator (pRetroX-Tet-On-Advanced) and the target construct driven by the transactivator (pRetroX-Tight-Pur plus the target gene). To implement this system, we first established rtTA transgene-expressing cell lines, including Hep3B, Renca, and MAD109. An important advantage of the Retro vector system in our protocol was the ability to monitor the expression and localization of the S protein over time and observe the effects of the expressed protein on the cell. Immunohistochemical (IHC) staining, without permeabilization, showed that the SARS-CoV-2 S protein was present in the cell membrane of Renca cells expressing S Δ21 in the presence of Dox (Fig. 1A). In contrast, the S protein could not be detected in the cell membrane of cells expressing S wt without permeabilization (Fig. 1B). Upon permeabilization, however, the S protein was observed in the cytoplasm of cells expressing SARS-CoV-2-S wt (Fig. 1B), indicating that it is expressed but remains within the cytoplasm. This

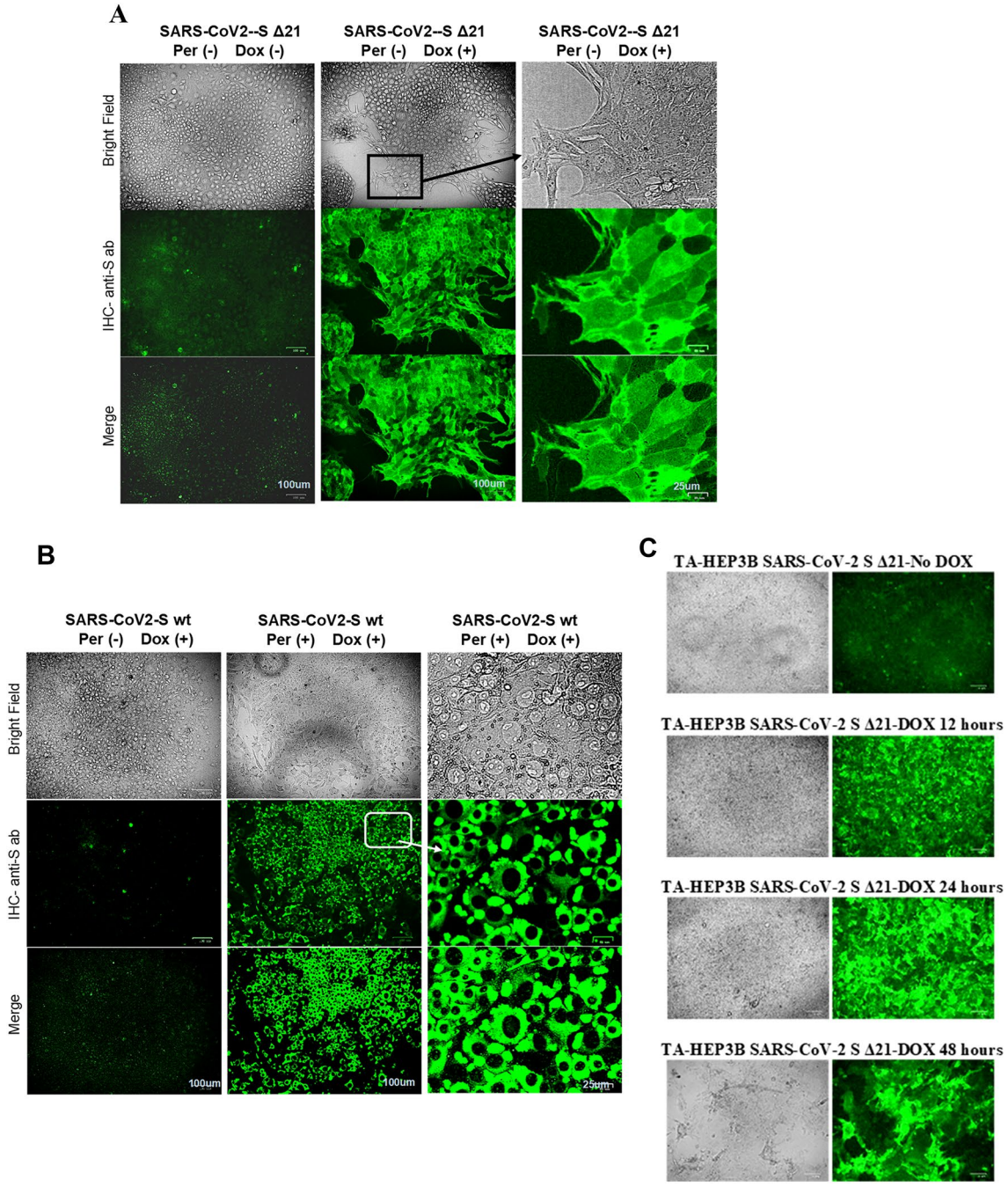

Fig. 1. Assessment of SARS-CoV-2 Spike Δ21 protein expression and localization in Renca and Hep3B cells using a doxycycline-inducible retroviral vector system. (**A**) Immunohistochemistry (IHC) was performed to assess the localization of SARS-CoV-2 Spike Δ21 protein in the Renca cell membrane after Dox induction. (**B**) IHC was conducted on Renca cells expressing wild-type (wt) SARS-CoV-2 Spike to determine localization in the cytoplasm. (**C**) Hep3B cells containing the pRetroX-Tight-Pur-hSARS-CoV2-S Δ21 construct were induced with doxycycline (Dox) at various time intervals, and IHC was performed to evaluate Spike protein expression and cell-cell fusion. Note: IHC tests were conducted without a permeabilization step. (**D**) Dot blot analysis was utilized to assess the presence of SARS-CoV-2 Spike Δ21 protein in the Renca cell membrane, confirming membrane localization. (**E**) ELISA was performed to quantify SARS-CoV2-S Δ21 expression levels in relation to the number of cells expressing the protein. (**F**) ELISA was conducted to evaluate SARS-CoV2-S Δ21 expression over time following Dox addition. Note: ELISA tests were performed without a permeabilization step. (**G**) Minimal signal detection was observed in Renca cells expressing SARS-CoV2-S wt. Control conditions are indicated as Per (-) for no permeabilization and Dox (-) for no doxycycline treatment. (ab) indicates primary antibody. See also Figures S1 to S4 for additional data.

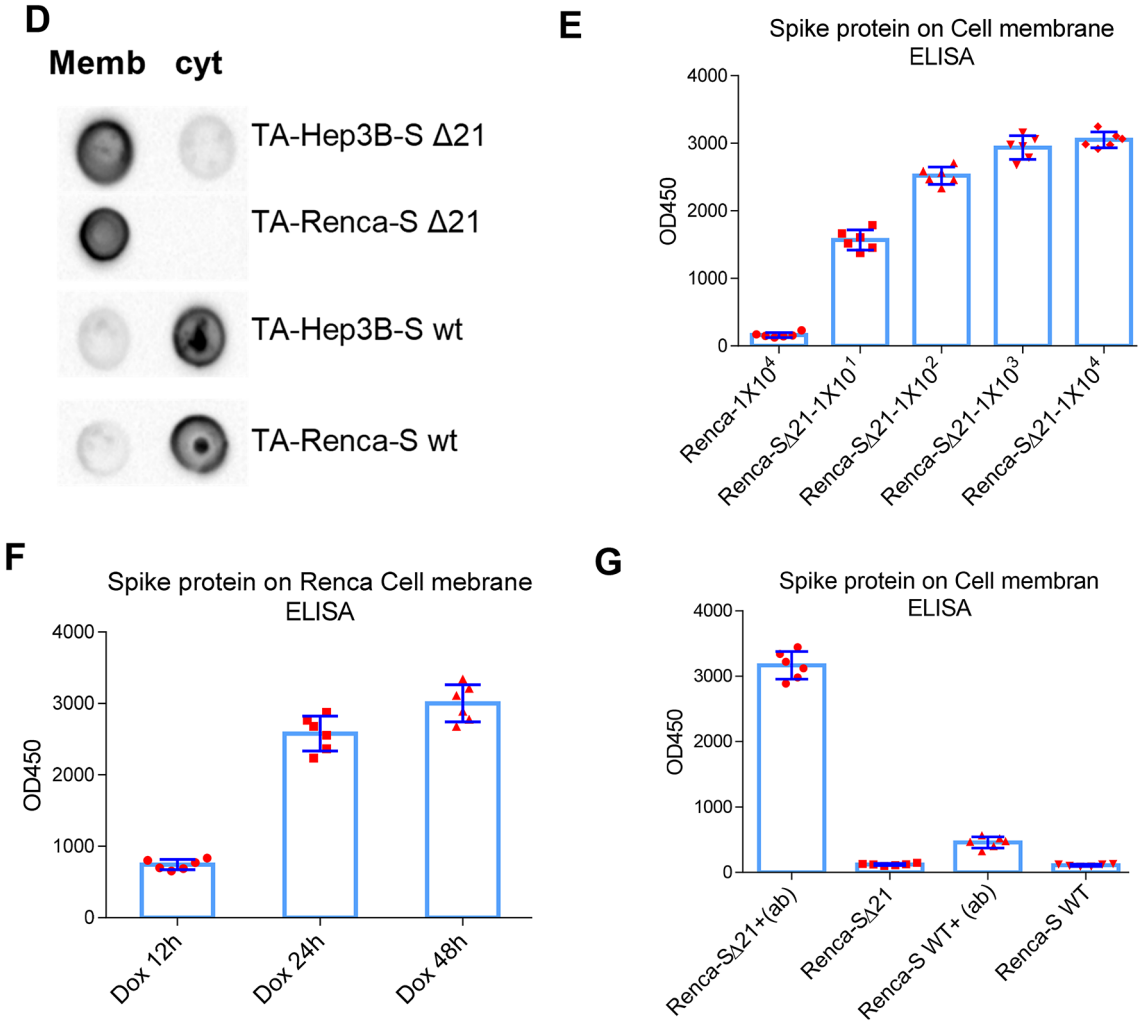

Figure 1. (continued)

suggests that without the 21 amino acid deletion, the wt-S protein does not function as a carrier to transport to the membrane.

Moreover, the amount of S protein in the cell membrane increased significantly in TA-Hep3B cells containing pRetroX-Tight-Pur-hSARS-CoV-2-S Δ21, as well as in TA-Renca and TA-MAD109 cells containing pRetroX-Tight-Pur-mSARS-CoV-2-S Δ21, with prolonged Dox induction. Validating these results across different cell types, such as human (Hep3B) and murine (Renca and MAD109) cell lines, ensures that the observed effects are not cell type-specific and supports the robustness and generalizability of our approach. This cross-validation is crucial for demonstrating the broader applicability of the method to various biological systems (Fig. 1C and Fig. S1A and B).

We further assessed the expression of the SARS-CoV-2 S protein on the cell membrane using a dot blot assay. Cell membrane isolation was confirmed by the absence of GAPDH and Cog2, which are primarily cytoplasmic, while calreticulin and calnexin were present in both the membrane and cytoplasm (Fig. S2). Dot blot results indicated that nearly all of the S protein was located in the cell membrane of cells expressing S Δ21, whereas little to no S protein was detected in the membrane of cells expressing S wt in both Hep3B and Renca cells (Fig. 1D).

It was previously demonstrated that the localization of the S protein on the cell membrane causes cell-cell fusion[10]. In our study, we observed dramatic cell-cell fusion in Hep3B cells expressing S Δ21 within 24 h of Dox addition. By 48 h, this fusion led to significant disruption of cell structure in Hep3B cells expressing S Δ21 (Fig. 1C). In cells expressing the wt S protein, almost no cell-cell fusion was observed, indicating that the full-length S protein, without the C-terminal deletion, does not reach the cell membrane (Fig. S3).

SARS-CoV-2 S Δ21 expression results in significant Spike protein localization on the cell membrane, as determined by ELISA

We investigated whether the SARS-CoV-2 S protein localized on the cell membrane could be detected using an ELISA assay with the same antibody used for IHC. TA-Hep3B and TA-Renca cells, expressing either S wt or S Δ21 vectors, were seeded into 96-well cell culture plates at densities ranging from 1×10^1 to 1×10^4 cells per well.

Doxycycline (Dox) was added after 24 h, and cells were fixed with 4% paraformaldehyde after 12, 24, and 48 h. The ELISA protocol was conducted without permeabilization.

The results showed a signal increase corresponding to the number of cells expressing S Δ21 and the duration of Dox treatment (Fig. 1E and F; Fig. S4A and B). In contrast, little or no signal was detected in Renca and Hep3B cells expressing S wt (Fig. 1G, Fig. S4C). Additionally, permeabilization increased the ELISA signal in cells expressing S wt, while no change was observed in cells expressing S Δ21 (Fig. S4D).

SARS-CoV-2 S Δ21 replaces native cell membrane proteins

During ELISA assays, we observed that human sera, regardless of the presence of SARS-CoV-2 S antibodies, produced 4–5 times higher signals in control cells (without ectopic S Δ21 expression) compared to Hep3B-S Δ21 or Renca-S Δ21 cells expressing SARS-CoV-2 S on the membrane. This was noted when using anti-IgG secondary antibodies (both human and mouse) prepared without affinity purification (Fig. S5 A, B, and C). To determine if this finding was cell-related, we conducted a background comparison using ELISA with anti-IgG secondary antibodies prepared with affinity purification; wells were coated with 20 ng of S1 protein, and no significant difference was observed between results with TA-Renca S Δ21 cells (Fig. S6).

These observations led us to hypothesize that the high expression of SARS-CoV-2 S Δ21 protein might replace native cell membrane proteins. To explore this, we examined the levels of Spectrin Alpha Erythrocytic1 (SPTA1), a scaffold protein linking the cell membrane to the actin cytoskeleton, and N-cadherin (CDH2), a transmembrane protein, in both the cell membrane and cytoplasm of cells with and without SARS-CoV-2 S Δ21 expression.

After 36 h of Dox treatment, we isolated cell membranes and cytoplasm from Hep3B and Renca cells expressing S Δ21 and controls. Dot blotting with specific antibodies for SPTA1 and CDH2 revealed that the levels of these proteins in the membranes of cells expressing S Δ21 were 2–3 times lower than in non-expressing cells (Fig. 2A and B).

To confirm these findings, we evaluated SARS-CoV-2 S protein expression (Fig. 2C) and the levels of SPTA1 and CDH2 by ELISA at 0, 12, 24, and 48 h after Dox addition (Fig. 2D and E). Our results showed that the decrease in SPTA1 and CDH2 levels corresponded to the increase in S protein levels in the cell membrane (Fig. 2C, D, and E). Additionally, ELISA using SARS-CoV-2 S-negative patient serum as an autoantibody source against the cell membrane yielded similar results (Fig. 2F).

Thus, overexpression of SARS-CoV-2 S Δ21 in cells leads to the transport of the S1 protein to the cell membrane, resulting in the replacement of native membrane proteins.

Vaccination with CM-S induces a more robust immune response than mRNA-S (BNT162b2, Pfizer-BioNTech)

As described above, CM-S consists of cell membranes that naturally incorporate the S protein. In this context, both the membrane and S protein are in their natural form, and the membrane-S protein complex is obtained directly from cell culture through simple and non-disruptive processes. One of the significant challenges in vaccination strategies is obtaining sufficient antigen, especially in protein format. With the CM-S format, a larger number of cells in culture can provide more S protein as antigen, and growing cells in large amounts is a relatively straightforward process. Importantly, vaccination with CM-S allows for direct local delivery in the intradermal space, facilitating immediate presentation to immune cells. In contrast, with the highlighted protocol, mRNA-lipid particles must first enter the cell, where S protein is expressed and undergoes various processing steps before being transported to the cell membrane for immune recognition. Additionally, once the membrane-S protein enters the bloodstream, its movement to other organs is limited due to the size of the membrane complex. Conversely, one of the challenges with mRNA-lipid particles is their ability to circulate in the bloodstream and reach other tissues, which may lead to unintended consequences.

We assessed the immune response in Balb/c and C57BL/6 mice vaccinated with cell membranes from cells expressing SARS-CoV-2 S Δ21 protein (CM-S). We standardized the amount of membrane-S protein (CM-S) complex based on the results shown in Fig. 1E and F. Specifically, the CM-S was obtained from a cell density of 5×10^4 cells, 36 h after the addition of doxycycline (DOX) to the cell culture. For the experiments, whole cells expressing SARS-CoV-2 S Δ21 were used after a similar 36-hour incubation following DOX addition, and the cells were subsequently isolated and washed in PBS. These standardized protocols were consistent for further experiments described below unless indicated otherwise.

Blood samples were collected from the tail vein 28 days after single and double vaccinations to measure antibody titers and perform virus neutralization assays. Total anti-SARS-CoV-2 S IgG antibody levels were quantified using ELISA. Mice immunized with a single dose of cell membrane from Renca cells expressing SARS-CoV-2 S with complete Freund's adjuvant (CFA) showed significantly higher endpoint titers of S protein-specific IgG compared to those receiving CM from Renca cells with CFA in both Balb/c (Fig. 3A) and C57BL/6 mice (Fig. 3B).

We also compared immune responses from CM-S and UV-killed whole Renca cells expressing SARS-CoV-2 S Δ21 (WhC-S). Mice immunized with Renca CM-S exhibited a slight, non-significant increase in S protein-specific IgG compared to those immunized with Renca WhC-S (Fig. 3C). Renca WhC (not expressing SARS-CoV-2 S Δ21) used as a background control produced significantly more signals than CM from Renca cells (Fig. 3C). Additionally, we examined the impact of Freund's adjuvant—used as complete in the first vaccination and incomplete in the second—on immune response induction. Mice receiving adjuvant with the initial CM-S vaccination showed significantly stronger S protein-specific immune responses. After the second vaccination, the response without adjuvant was nearly equivalent to that with adjuvant (Fig. 3D).

We then compared immune responses from the CM-S vaccination with those from the mRNA COVID-19 vaccine (BNT162b2, Pfizer-BioNTech) and the whole inactivated virus (WIV) vaccine. The mice were immunized

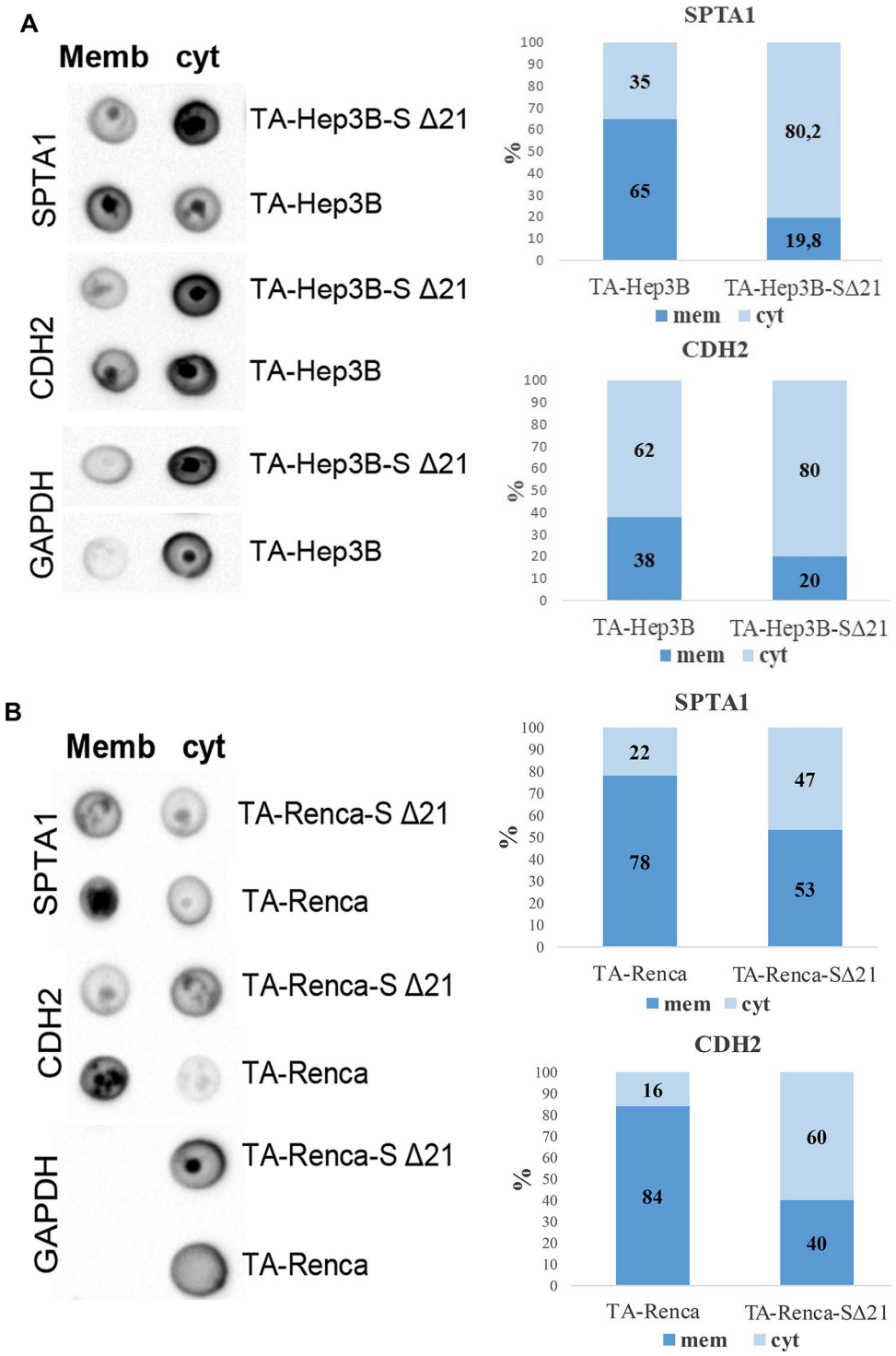

Fig. 2. Examination of native cell membrane protein levels, including SPTA1 and CDH2, in cells expressing SARS-CoV-2 S Δ21. Cell membranes and cytoplasmic fractions were isolated from TA-Hep3B (control) and TA-Hep3B containing pRetroX-Tight-Pur-hSARS-CoV2-S Δ21, as well as TA-Renca (control) and TA-Renca containing pRetroX-Tight-Pur-mSARS-CoV2-S Δ21 cells, after 36 h of doxycycline (Dox) treatment. The levels of SPTA1 and CDH2 proteins in both the cell membrane and cytoplasm were assessed using dot blot with specific antibodies for SPTA1 and CDH2. (**A**) Dot blot analysis and corresponding graphs depict the abundance of SPTA1 and CDH2 proteins in the cytoplasm and membranes of Hep3B cells. (**B**) Dot blot analysis and corresponding graphs show the abundance of SPTA1 and CDH2 proteins in the cytoplasm and membranes of Renca cells. Following Dox addition, the expression levels of SARS-CoV-2 S protein (**C**), CDH2 membrane protein (**D**), and SPTA1 cell membrane protein (**E**) were evaluated by ELISA at 0, 12, 24, and 48 h in Renca cells expressing SARS-CoV2-S Δ21. (**F**) ELISA results using SARS-CoV-2 S-negative patient serum as a source of autoantibodies against the cell membrane are also presented.

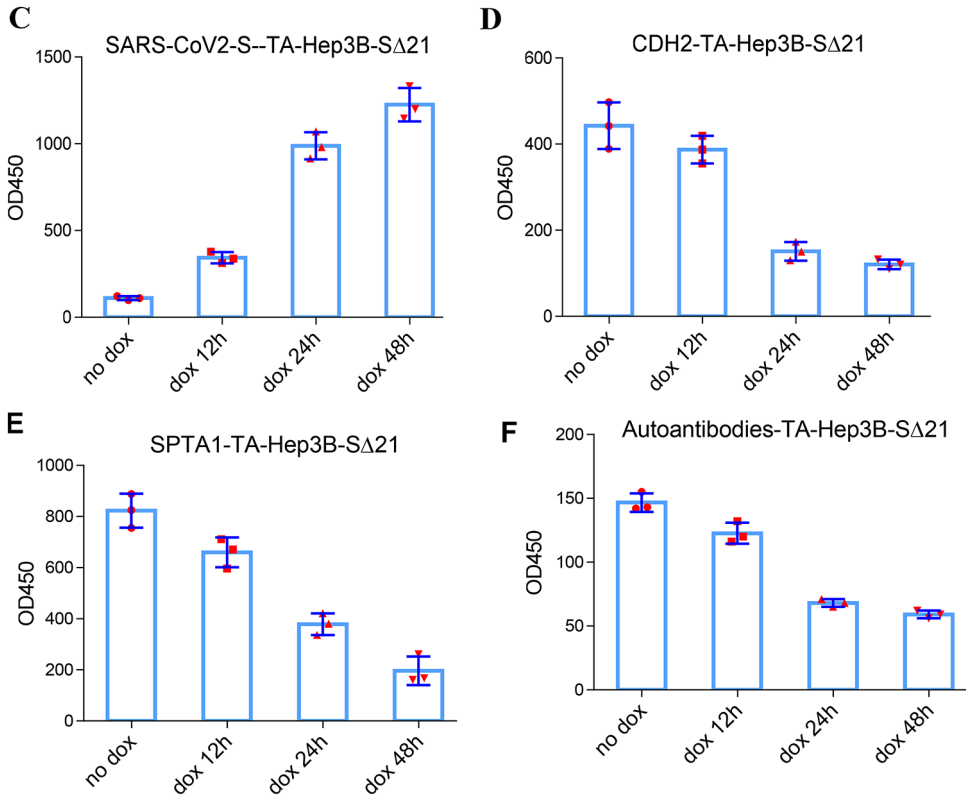

Figure 2. (continued)

with the defined dose of the Pfizer-BioNTech COVID-19 mRNA S vaccine (BNT162b2) as specified for adult humans. Additionally, the mice received the whole inactivated virus (WIV) using the same immunization protocol recommended by the manufacturer, with dosing also aligned to that described for adult humans. Under identical conditions, CM-S vaccination elicited a statistically more robust immune response than mRNA-S vaccination (BNT162b2) (Fig. 3E). This difference was particularly pronounced after a single-dose vaccination (Fig. 3E and F). Furthermore, CM-S vaccination also generated a stronger immune response compared to human sera from individuals vaccinated with BNT162b2 (mRNA-S-PS) and convalescent COVID-19 patients (hcPS) (Fig. 3F).

CM-S vaccination produces more SARS-CoV-2 neutralizing antibodies

We measured anti-SARS-CoV-2-neutralizing antibodies in the serum of vaccinated mice using a method specifically developed for this study. This method involves removing S protein-specific antibodies from serum by binding them to cells presenting the SARS-CoV-2 S protein (WhC-S) on their membrane, as detailed in the materials and methods section (Fig. 4A). Additionally, the sera from vaccinated mice were tested with a live SARS-CoV-2 neutralization assay. All neutralization tests were conducted using sera collected after the booster dose. The sera from vaccinated mice and humans, diluted two-fold, were neutralized using Renca cells expressing the SARS-CoV-2 S protein (WhC-S) on their membrane, and mean endpoint titers were determined for relative comparisons.

Neutralization tests with cells expressing the SARS-CoV-2 S protein (WhC-S) indicated that the mean endpoint titers of S protein-specific IgG in mice immunized with CM-S were 6.2-, 2.7-, and 2.6-fold higher than those in mice double-vaccinated with mRNA-S, human sera double-vaccinated with BNT162b2, and convalescent human sera (hcPS), respectively (Fig. 4B).

Consistent with these findings, live SARS-CoV-2 neutralization assays demonstrated a statistically significant difference in neutralizing antibody levels in mice receiving double vaccination with CM-S compared to those double-vaccinated with mRNA-S and WIV (Fig. 4B). The mean NT50 (50% neutralization titers) values for CM-S were 7-fold higher than those observed in the sera of mice double-vaccinated with mRNA-S (Fig. 4C). The live SARS-CoV-2 neutralization assays were conducted as a single-blinded experiment.

CM-S vaccination provides balanced Th1/Th2 immune response

In humans, induced virus neutralization is the gold standard for assessing vaccine efficacy. However, in mouse models, the detection of IgG, IgG1, and IgG2a antibody titers, along with the IgG1/IgG2a ratio, offers a better correlation with the Th1/Th2 immune response, SARS-CoV-2 vaccine efficacy, and protective capability than neutralization alone[11,12]. An increased IgG1/IgG2a ratio indicates a Th2-type humoral immune response, while an increased IgG2a/IgG1 ratio suggests a Th1-type cellular immune response. A balanced Th1/Th2 immune

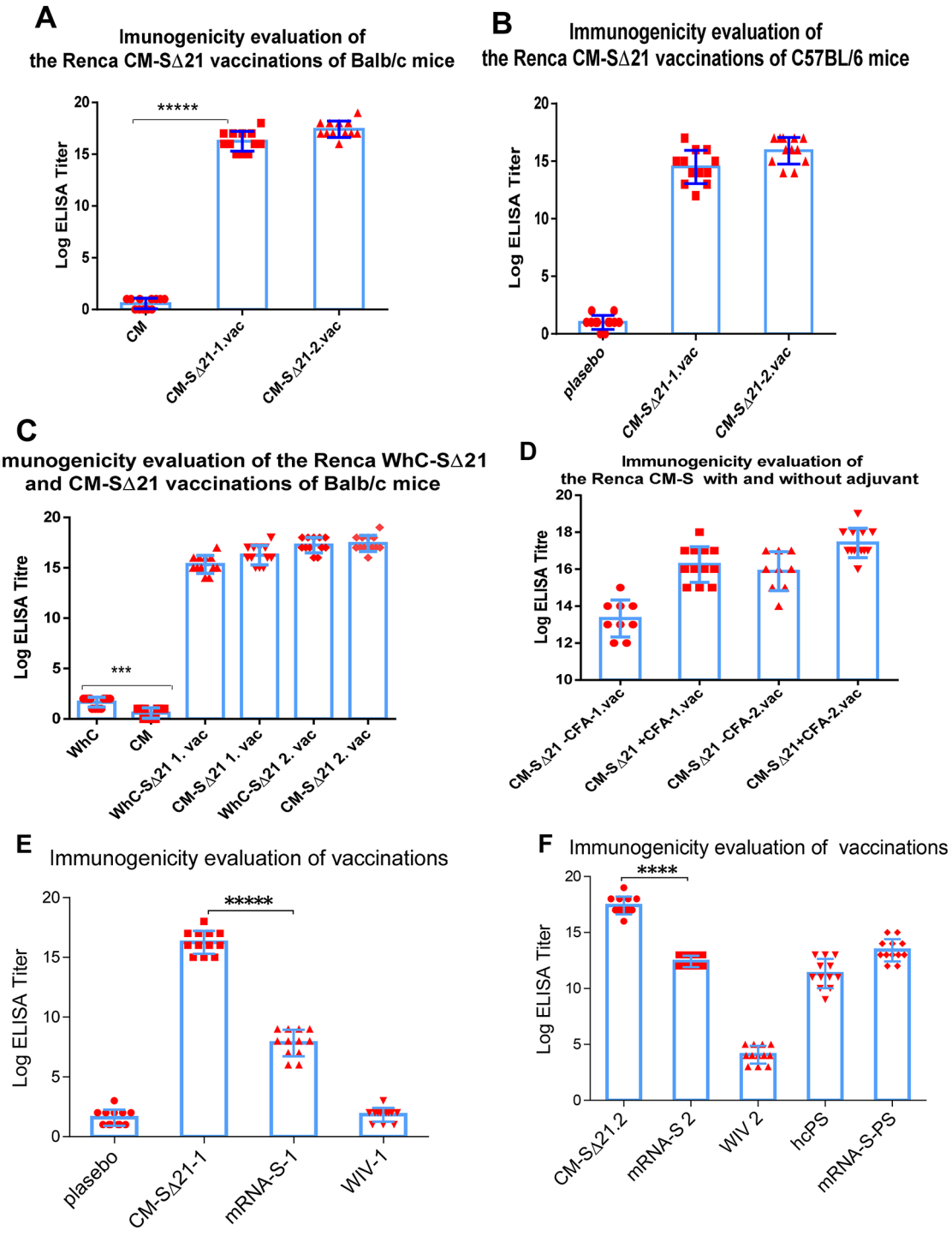

response (IgG1/IgG2a ratio close to 1) enhances the vaccine's protective effect and helps avoid pathological enhancement post-immunity.

We measured the mean endpoint titers of IgG1 and IgG2a in mouse sera from mice vaccinated with CM-S, mRNA-S, and WIV, using ELISA plates coated with the SARS-CoV-2 S protein. Results showed that CM-S vaccination elicited 4.2 and 4.9-fold more IgG1 than mRNA-S and WIV vaccinations, respectively. Similarly, CM-S induced 4.3 and 3.2-fold more IgG2a than mRNA-S and WIV vaccinations, respectively (Fig. 5A-C). Importantly, CM-S vaccination produced a more balanced Th1/Th2 immune response compared to mRNA-S and WIV vaccinations (Table 1).

SARS-CoV-2 S Protein-Cell membrane Immunogenic composition does not induce inflammatory cytokine response in mice

Some vaccine candidates can trigger uncontrolled cytokine release due to their structure or the adjuvants used with them[9,13]. Ideally, a vaccine should prevent or at least not cause the release of harmful cytokine levels. We evaluated 13 cytokine responses associated with inflammation and both innate and adaptive immunity in the

Fig. 3. Immunogenicity evaluation of SARS-CoV-2 S Δ21 cell membrane vaccine (CM-S) compared to mRNA-S (BNT162b2) and whole inactivated virus (WIV) vaccines in Balb/c and C57BL/6 mice. (**A**) Serum IgG levels were analyzed in Balb/c mice after single (1) and double (2) vaccinations with Renca cell membrane (CM-S) expressing mSARS-CoV2-S Δ21, collected 28 days post-vaccination. (**B**) Serum IgG levels were measured in C57BL/6 mice after single (1) and double (2) vaccinations with Renca CM-S expressing mSARS-CoV2-S Δ21, collected 28 days post-vaccination. (**C**) Serum IgG levels were assessed in Balb/c mice after single and double vaccinations with Renca CM-S or whole Renca cells (WhC) expressing mSARS-CoV2-S Δ21, collected 28 days post-vaccination. (**D**) Serum IgG levels were evaluated in Balb/c mice vaccinated with Renca CM-S with and without adjuvant, collected 28 days post-vaccination. (**E**) Serum IgG levels from mice vaccinated with a single dose of CM-S were compared to those from mice vaccinated with mRNA-S (BNT162b2) and whole inactivated virus (WIV) vaccines. (**F**) Serum IgG levels following the booster dose of CM-S vaccination were compared with those from mRNA-S, WIV, human convalescent sera (hcPS), and human sera from individuals vaccinated twice with BNT162b2 (mRNA-S-PS). IgG titers were calculated as means ± SEM (standard error of the mean). Comparisons were performed using Student's t-test (paired, two-tailed). Data represent results from three independent experiments. Statistical significance is indicated as follows: **** < $p = 0.0001$, ***** < $p = 0.00001$, ****** < $p = 0.000001$.

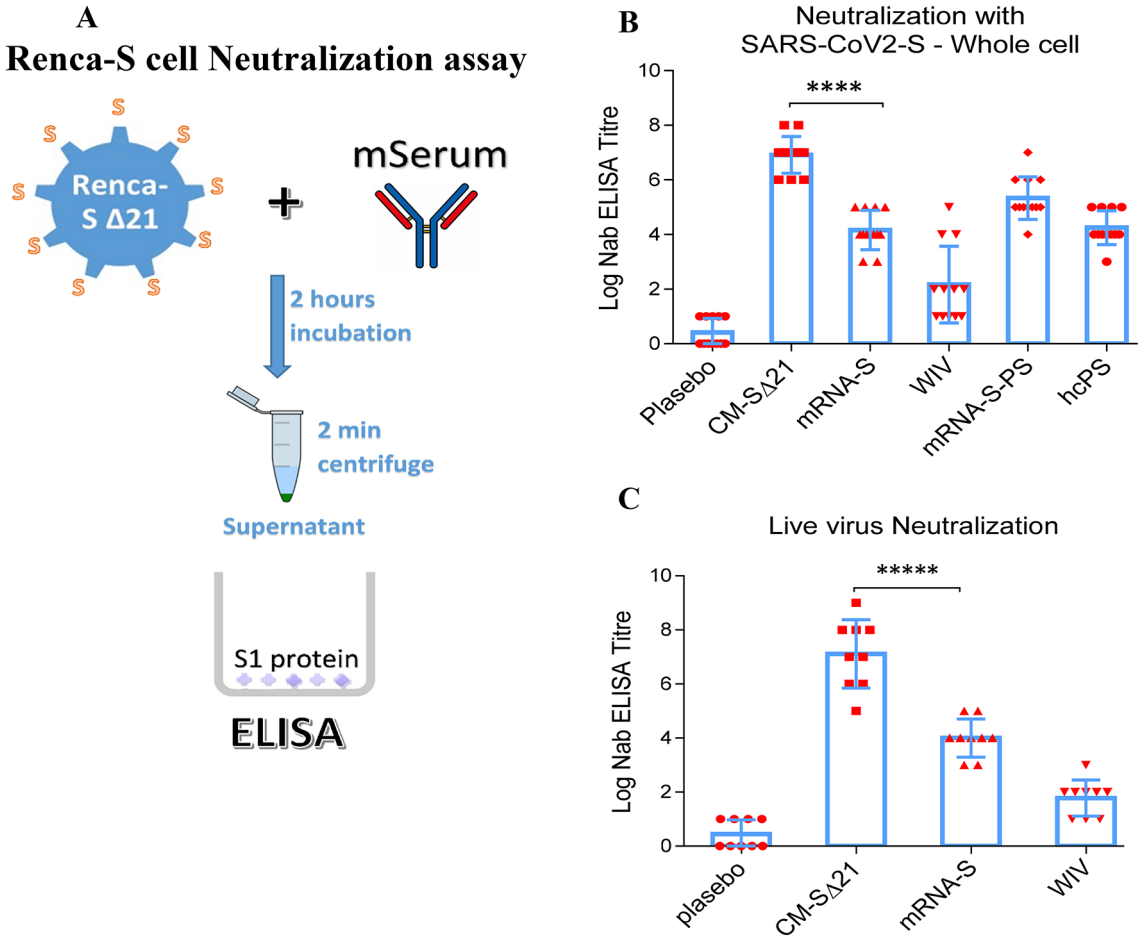

Fig. 4. Assessment of SARS-CoV-2 neutralizing antibodies in serum of Balb/c mice vaccinated with cell membrane vaccine (CM-S), mRNA vaccine (mRNA-S), whole inactivated virus (WIV), human convalescent sera (hcPS), or human sera vaccinated twice with BNT162b2 (mRNA-S-PS). (**A**) Schematic representation of the neutralization assay using Renca cells expressing SARS-CoV-2 S protein (WhC-S) to measure anti-SARS-CoV-2-specific antibodies in serum samples. Serum samples were processed to remove S protein-specific antibodies by binding them to WhC-S cells, as detailed in the materials and methods section. (**B**) Neutralization assays were conducted using cells presenting SARS-CoV-2 S protein on their membranes to determine mean endpoint titers of neutralizing antibodies in sera from vaccinated mice. (**C**) Neutralization assays using live SARS-CoV-2 virus were performed to assess the neutralizing capacity of serum from vaccinated mice. The mean NT50 (50% neutralization titers) values were calculated for each group. Statistical significance is indicated as follows: ** < $p = 0.01$, *** < $p = 0.001$, **** < $p = 0.0001$, ***** < $p = 0.00001$. Data are presented as means ± SEM (standard error of the mean). Comparisons were performed using Student's t-test (paired, two-tailed). Data represent results from three independent experiments.

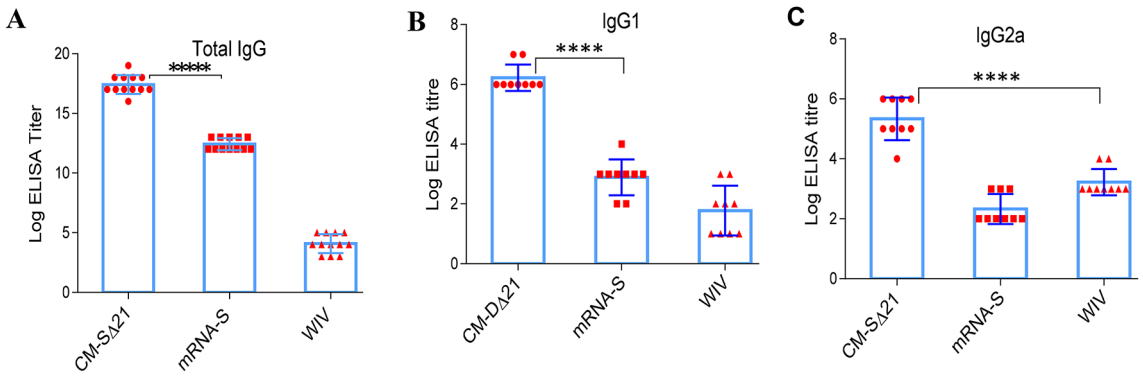

Fig. 5. Investigation of total IgG, IgG1, and IgG2a antibody levels and comparison of IgG2a/IgG1 ratios in mice vaccinated with cell membrane vaccine (CM-S), mRNA vaccine (mRNA-S), or whole inactivated virus (WIV). (**A**) Measurement of total IgG levels in mouse sera from the different vaccination groups, assessed using ELISA plates coated with SARS-CoV-2 S protein. (**B**) Measurement of IgG1 levels in mouse sera from the different vaccination groups, assessed using the same ELISA method. (**C**) Measurement of IgG2a levels in mouse sera from the different vaccination groups, assessed using ELISA. Table 1 summarizes the IgG2a/IgG1 ratios for each vaccination group. Statistical significance is indicated as follows: ** < $p = 0.01$, *** < $p = 0.001$, **** < $p = 0.0001$, ***** < $p = 0.00001$. Data are presented as means ± SEM (standard error of the mean).

Vaccine	IgG2a/IgG1
CM-SΔ21	0.87
mRNA-S	0.80
WIV	1.78

Table 1. The table displays comparison of IgG2a/IgG1 ratios in mice vaccinated with CM-S, mRNA-S, or WIV.

sera of control and vaccinated mice two weeks after the second CM-S vaccine dose. Additionally, we assessed cytokine secretion from the spleen cells of both control and vaccinated mice.

A key finding is that 12 out of 13 cytokines did not increase in the sera of mice that received two vaccine doses compared to controls two weeks post-vaccination. IL-17 A, among the 13 cytokines analyzed, showed a slight elevation (28%) in the serum of vaccinated mice (Fig. 6A-E and Fig. S7 A-J). Furthermore, levels of IL-1β, IL-6, IL-23, IL-27, MCP-1, and INF-β, primarily involved in inflammation, were reduced in the sera of vaccinated mice.

However, when examining splenocyte cells (mainly T and B lymphocytes, dendritic cells, and macrophages) from vaccinated and unvaccinated control mice, we found that splenocytes from vaccinated mice secreted significantly more IL-6, IL-17 A, IFN-γ, and TNF-α compared to those from unvaccinated mice (Fig. 6A-E and Fig. S7 A-J).

We monitored vaccinated mice's body weight, food and water intake, and clinical observations, including skin, fur, eyes, mucous membranes, secretions, excretions, and changes in gait and posture, over four months. No differences were observed compared to control mice.

The SARS-CoV-2 S Protein-Cell membrane composition provides Immunologic memory

Immunologic memory, primarily composed of T and B memory cells, is a hallmark of vaccination and is essential for successful immunization[14]. The immunologic response of T and B cells and the subsequent maintenance of memory cells are influenced by cytokines[15,16]. Assessing the immunologic memory induced by priming the immune system with pathogens or their cognate antigens is crucial in evaluating vaccine candidates. Therefore, we investigated cytokine secretion from splenocyte cells obtained from mice vaccinated with CM-S, both in the presence and absence of the SARS-CoV-2 S1 protein.

Consistent with the hypothesis that S1 protein enhances cytokine secretion in splenocytes from CM-S vaccinated mice, a significant correlation was found between the two groups (CM-S vaccinated and S1-primed splenocytes versus CM-S vaccinated and non-S1-primed splenocytes), with a p-value of 0.01 using the Wilcoxon Signed Ranks Test (Fig. 6E, F, G and Fig. S7 B-J). Although S1 protein significantly increased cytokine secretion in splenocytes overall, it only significantly increased IL-6, IL-17 A, IFN-γ, and IL-23 levels when analyzed individually compared to cells without S1 protein (Fig. 6A-G, and Fig. S7 A-J).

Importantly, the presence of S1 protein reduced all cytokines examined in splenocyte cells from vaccinated mice that were not S1 primed ($p = 0.001$, Wilcoxon Signed Ranks Test) (Fig. 6G and Fig. S7 B-J). It is important to note that the S1 protein used was preserved in a carrier-free environment and did not contain sodium azide or other chemicals.

Δ21 deleted Spike mRNA elicits a stronger immune response than wild type Spike mRNA

In a subsequent study, we explored whether using Δ21 deleted Spike mRNA (mRNA-SΔ21) instead of the complete spike mRNA (mRNA-Swt) used in current vaccines like BNT162b2 (Pfizer-BioNTech) would elicit a stronger immune response. Live Renca cells containing either pRetroX-Tight-Pur-mSARS-CoV2-S wt or pRetroX-Tight-Pur-mSARS-CoV2-S Δ21 were treated with doxycycline (dox) for 24 h in vitro and then administered subcutaneously in mice (Fig. 7A). To maintain S wt mRNA or S Δ21 mRNA expression, dox was added to the mice's drinking water. We assessed IgM and IgG immune responses in the two groups of animals on day 14. Our results indicated that mice injected with cells expressing SΔ21 exhibited twice the immune response compared to those injected with cells expressing S wt (Fig. 7B, C).

Furthermore, vaccinated mice and human sera, diluted two-fold, were neutralized using Renca cells expressing the SARS-CoV-2 S protein (WhC-S) on their membrane, and mean endpoint titers were measured for relative comparisons. It was found that the neutralizing antibody titer in the serum of mice administered mSARS-CoV2-S Δ21-expressing cells was higher than that of mice given mSARS-CoV2-S wt-expressing cells (Fig. 7D).

Vesicular stomatitis virus G protein (VSV-G) can facilitate membrane transport of SARS-CoV-2 S protein

In this study, we examined whether plasma membrane proteins like Vesicular Stomatitis Virus G (VSV-G) protein, similar to the SARS-CoV-2 S protein, can execute the same transport function. We removed the transmembrane domain (TM) of the S protein, including its C-terminal region, and replaced it with the TM region of the VSV-G protein (Fig. 8A). We then investigated the expression of the SARS-CoV-2 S protein in the membrane of cells expressing either SARS-CoV-2-SΔTM-VSV-G-TM (a hybrid protein with the VSV-G TM domain added to the S protein lacking its TM domain) or SARS-CoV-2-SΔTM (with the TM region removed). The genes for these proteins were overexpressed using vector systems designed for tetracycline-inducible retroviral mammalian expression under dox control in the culture medium.

Immunohistochemical (IHC) staining, performed without permeabilization, showed that the SARS-CoV-2 S protein was located in the cell membrane of cells expressing SΔTM-VSV-G-TM, whereas it was only present in the cytoplasm of cells expressing SΔTM (Fig. 8B and C, and Fig. S8). Similarly, in ELISA assays conducted without permeabilization, the S protein was found in the cell membrane of cells expressing SΔTM-VSV-G-TM, while cells expressing SΔTM showed little to no signal. It was also determined that the SΔTM-VSV-G-TM hybrid structure localized the spike protein on the cell membrane as effectively as the SARS-CoV-2-S Δ21 protein structure (Fig. 8D).

Additionally, we demonstrated that, similar to the expression of the SARS-CoV-2-S Δ21 protein, the membrane localization of the SΔTM-VSV-G-TM hybrid protein led to a reduction of the natural membrane protein SPTA1 in the membrane (Fig. 8E).

Discussion

Recently, the use of exosomes—nano-sized membrane vesicles capable of transferring proteins—in cancer vaccines has gained significant attention[17]. Challenges in exosome purification have led to the development of exosome mimetics, which are nanoparticles transported in cell membranes that simulate exosomes.

The method described in this study focuses on the transport of the S protein by incorporating it into the cell membrane in its most natural form, facilitating antigen presentation and inducing an immune response.

Antigen preparation has often posed challenges in antibody production, primarily due to insufficient antigen quantities for mammalian immunization and inadequate purification. The use of baculovirus systems has garnered interest for expressing large quantities of protein on the baculovirus membrane. However, this approach also results in the expression of baculovirus-derived membrane proteins alongside foreign membrane proteins.

Using the method described in this study, it is possible to produce an almost unlimited amount of SARS-CoV-2 S antigen in its native form using cell membranes quickly and cost-effectively.

Whole dead tumor cell (autologous or allogeneic) vaccinations have been tested in cancer patients for a long time, with clinical applications approved and in use[18]. Using cell membranes results in a more specific immune response compared to whole cells, as it reduces the potential for non-specific immune responses (Fig. 3C).

An important finding of this study is the significant reduction of native cell membrane proteins and their replacement by the SARS-CoV-2 S protein, which prevents the formation of unwanted background antibodies and enhances immune specificity. Furthermore, this method generates an effective immune response without the need for adjuvants, particularly following the second vaccination.

Another important advantage of this method is that the attachment of the S protein to the cell membrane may prevent its free circulation, thereby reducing the likelihood of crossing the blood-brain barrier. This could mitigate the risk of cell signal stimulation effects that contribute to complex cardiovascular outcomes, as reported in studies related to other vaccination methods[19,20]. Notably, unlike mRNA vaccines, the membrane-embedded S protein used in this method does not need to enter the cell, thereby minimizing potential issues within cells and organs.

The significantly greater stability of proteins compared to mRNA allows this vaccination system to be stored for extended periods at -20 °C, and even at +4 °C for specific durations. Additionally, the combination of the S protein with membrane lipids helps maintain the integrity of the S protein for longer periods than when the protein is present alone.

Some vaccines may cause an uncontrolled cytokine storm in certain vaccinated individuals, potentially leading to acute respiratory distress syndrome (ARDS), a common cause of death in COVID-19 patients[9]. This study demonstrated that the SARS-CoV-2 S protein-cell membrane immunogenic composition does not

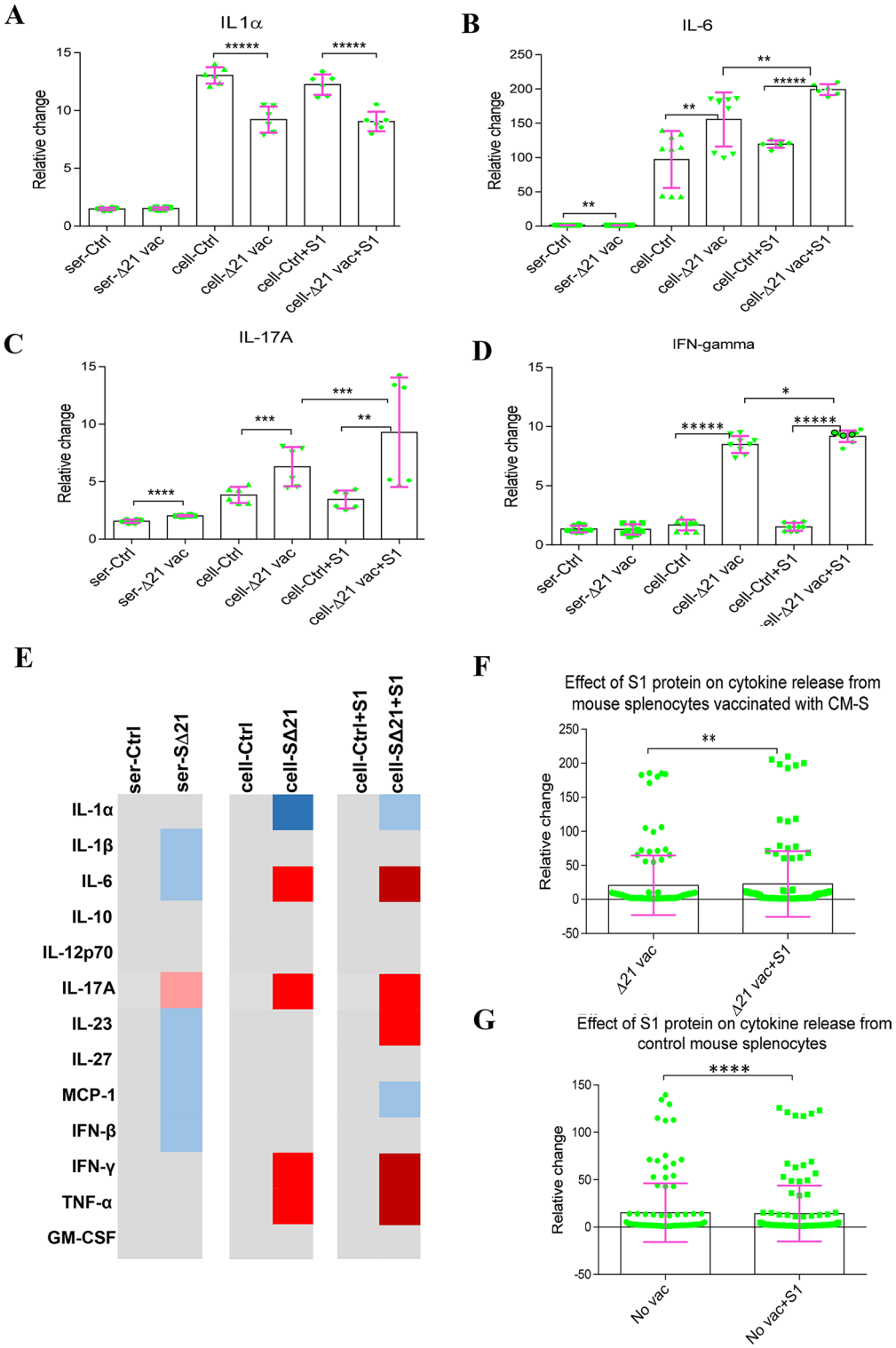

trigger uncontrolled cytokine release in mice in vivo. In our cytokine response study, we found that 12 out of 13 cytokines were not elevated in the sera of mice vaccinated with two doses compared to controls. Furthermore, levels of IL-1β, IL-27, MCP-1, and INF-β, which are primarily involved in inflammation, were decreased in the sera of vaccinated mice.

Beyond the cytokine response, the absence of abnormalities in clinical observations for more than six months after the final vaccination suggests that this vaccination method did not harm the host.

Evaluating the immunologic memory induced by priming the immune system with pathogens or their specific antigens is crucial for assessing vaccine candidates[16]. The immunologic response of T and B cells, and the subsequent maintenance of memory cells, are influenced by cytokines[15,16]. This study, using the Wilcoxon Signed Ranks correlation test, demonstrated that the S1 protein enhances the overall cytokine response in the splenocytes of vaccinated mice (Fig. 6E).

◀**Fig. 6**. Evaluation of cytokine responses in sera from CM-S-vaccinated and unvaccinated control mice, and assessment of immunologic memory in splenocyte cells in the presence and absence of SARS-CoV-2 S1 protein. (**A**-**D**) Cytokine responses measured in the sera of vaccinated and unvaccinated mice: (**A**) IL-1α, (**B**) IL-6, (**C**) IL-17 A, and (**D**) IFN-γ levels secreted from splenocyte cells. (**E**) Summary of all cytokine responses as pairwise comparisons. In comparison groups, gray indicates no change, increases are indicated in red, and decreases in blue. The intensity of the colors represents the magnitude of changes; all indicated changes were statistically significant with $p > 0.05$. Ser-SΔ21 refers to sera from CM-S-vaccinated mice, while Ser-Ctrl refers to sera from unvaccinated control mice. Cell-SΔ21 denotes splenocyte cells obtained from the spleens of CM-S-vaccinated mice, and Cell-Ctrl refers to splenocytes from unvaccinated mice. S1 refers to the S1 subunit of the SARS-CoV-2 S protein. (**F**) Correlation between the two groups supporting the hypothesis that S1 protein increases cytokine secretion, assessed using the Wilcoxon Signed Ranks Test. (**G**) Correlation between the two groups supporting the hypothesis that S1 protein decreases cytokine secretion, also evaluated with the Wilcoxon Signed Ranks Test. Statistical significance is indicated as follows: ** < $p = 0.01$, *** < $p = 0.001$, **** < $p = 0.0001$, ***** < $p = 0.00001$. See also Figures S7.

Upon stimulation with the cognate antigen, SARS-CoV-2 S1 protein, it was observed that splenocytes from mice inoculated with CM-S and stimulated with the SARS-CoV-2 S1 protein secreted significantly more IL-6, IL-17 A, IFN-γ, and IL-23 cytokines compared to vaccinated but unstimulated splenocytes. Importantly, these cytokines, which are increased in the presence of the S1 protein, play critical roles in both innate and adaptive immunity against viral infections and have the ability to directly inhibit viral replication. The S1 protein alone did not alter the secretion of inflammation-related cytokines, including IL-1β, IL-27, MCP-1, and INF-β, which were found to be decreased in the serum of vaccinated mice.

Interestingly, the S1 protein reduced all cytokines examined in splenocyte cells from vaccinated, non-S1 primed mice (Fig. 6F). The ACE2/Angiotensin-(1–7)/Mas Receptor Axis is known for its anti-inflammatory potential and ability to inhibit cytokine release[21]. Accordingly, we found that the S1 protein decreased nearly all 13 cytokines secreted from splenocyte cells of mice that had not previously encountered the SARS-CoV-2 S protein. Since the SARS-CoV-2 S protein does not bind to the mouse ACE2 receptor, it remains unclear how the S1 protein reduces cytokine secretion from splenocytes in mice that have not been previously exposed to CM-S. These findings suggest the potential use of the S1 protein alone in the prevention of cytokine release and treatment of cytokine storms.

Although the present study described the S2 subunit of the SARS-CoV-2 S protein and VZV-G as antigenic protein carriers, different DNA sequences of plasma membrane proteins, such as influenza hemagglutinin, respiratory syncytial virus (RSV) fusion glycoprotein (F), and human immunodeficiency virus gp160 (env) proteins, analogous to the SARS-CoV-2 S protein, could also perform similar transportation functions.

Importantly, this method can be applied not only as a COVID-19 vaccination but also for vaccination against other microbial agents, including viruses and bacteria, and even for cancer treatment. This is achieved by combining any protein or epitope with antigenic properties, including tumor-associated antigens, with the S2 Δ21 subunit, which serves as a carrier to the cell membrane.

In addition to the new findings mentioned above, we also demonstrate that using the SARS-CoV-2 Spike mRNA-based vaccination method (S Δ21 mRNA) may offer a more effective vaccination strategy, eliciting improved responses in patients.

While we emphasize the use of the antigen-membrane structure as a vaccine, the neutralization test described in this study—comparable in sensitivity to live virus neutralization—is one of the significant findings (Fig. 4A). Furthermore, it is evident that ELISA applications or antibody production using cells that express antigens intensively on the membrane will be much simpler and more cost-effective than existing methods.

Materials and methods

Cells

Human Hep3B (ATCC-HB-8064), mouse Renca (ATCC-2947), MAD109 (mouse lung cancer-gift from Dr. Alan L. Epstein) cell lines were used. The cells were grown in DMEM or RPMI medium supplemented with 10% FBS, 1% Penicillin/Streptomycin, 1% L-glutamine. All cells were incubated at 37 °C, 5% CO2 conditions.

Mouse and human codon optimized SARS-CoV-2-S-wt and -Δ21 cDNA preparation

SARS-CoV-2 strain Wuhan-Hu-1 (GenBank NC_045512) spike genome was codon-optimized to mouse (mSARS-CoV-2 S wt) and prepared as mSARS-CoV-2 S wt and mSARS-CoV-2 S Δ21 by GenScript (https://www.genscript.com). Codon optimized to H. sapiens SARS-CoV-2-S-wt was a gift from Gerald Pao (Addgene plasmid #141347; http://n2t.net/addgene:141347; RRID: Addgene_141347). Codon optimized to H. sapiens SARS-CoV-2-S-Δ21 was a gift from Jesse Bloom (Addgene plasmid #155130; http://n2t.net/addgene:155130; RRID: Addgene_155130).

Overexpression of SARS-CoV-2-S Wt and -SΔ21 using the Retro-X Tet-On advanced inducible expression system in cells

The Retro-X Tet-On Advanced Inducible Expression System requires the simultaneous presence of two retroviral constructs in a cell: the tetracycline-dependent rtTA transactivator (pRetroX-Tet-On-Advanced) and the target construct driven by the transactivator (pRetroX-Tight-Pur plus target gene). Thus, we first established rtTA transgene-expressing Hep3B, Renca, and MAD109 cell lines. For this purpose, HEK293T cells were transfected with the pRetroX-Tet-On-Advanced and helper vectors pCMV-VSV-G, pUMVC, using the CalPhos Mammalian

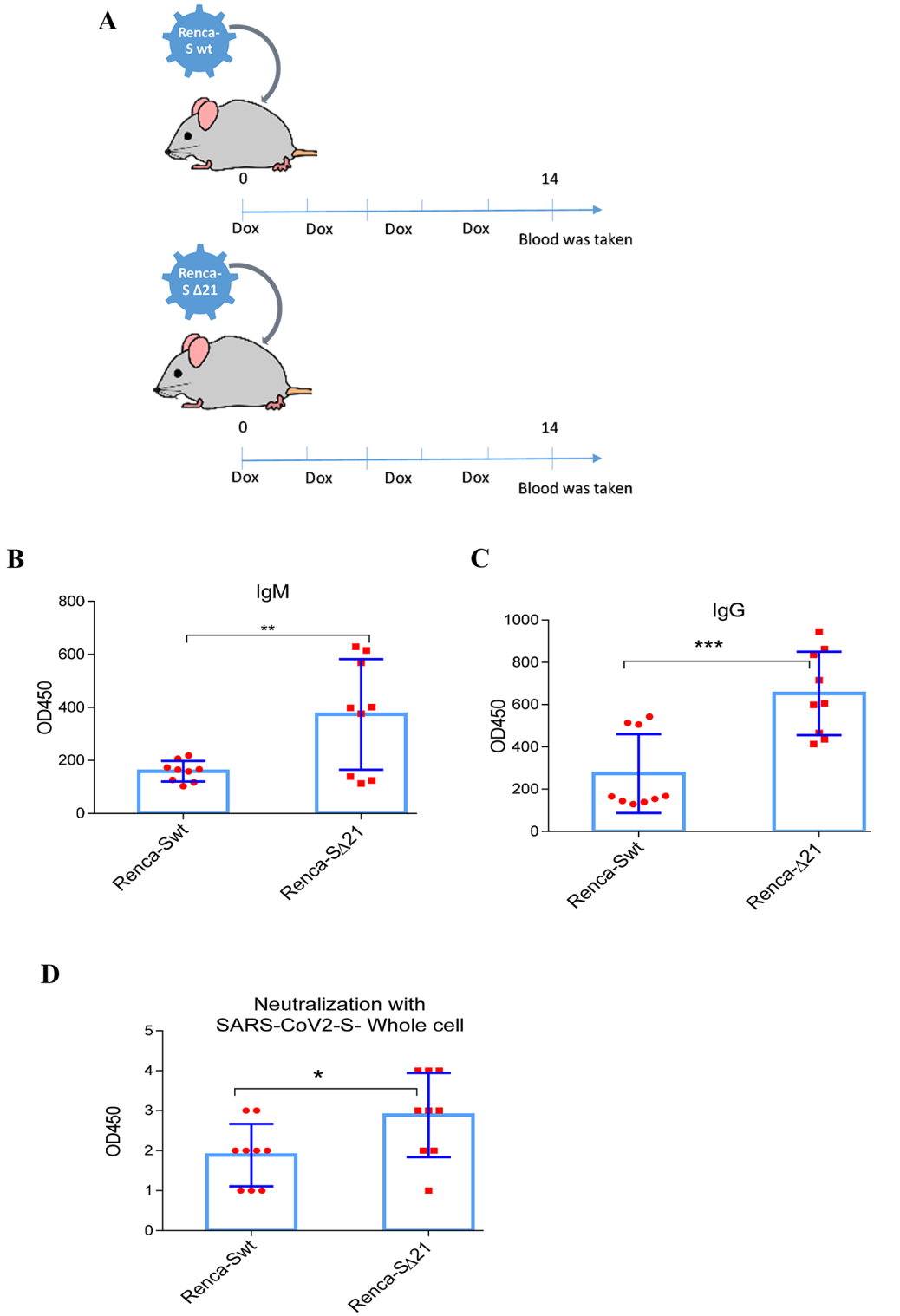

Fig. 7. Comparison of immune responses elicited by subcutaneous administration of live Renca cells expressing mRNA-based SARS-CoV-2 Spike S Δ21 and wild-type Spike (S wt) mRNA, with doxycycline treatment for expression maintenance. (**A**) Schematic representation of the establishment of SARS-CoV-2 Spike S wt or S Δ21 mRNA-protein expression in mice following subcutaneous administration of live Renca cells containing pRetroX-Tight-Pur-mSARS-CoV2-S wt or pRetroX-Tight-Pur-mSARS-CoV2-S Δ21, with doxycycline (dox) treatment for 24 h in vitro and subsequent dox addition to drinking water for expression maintenance. (**B**) Comparison of IgM levels in the sera of mice injected with cells expressing S wt or S Δ21 mRNA. (**C**) Comparison of IgG levels in the sera of mice injected with cells expressing S wt or S Δ21 mRNA. (**D**) Measurement of neutralizing antibody titers in the sera of mice administered mSARS-CoV2-S Δ21-expressing cells compared to those given mSARS-CoV2-S wt-expressing cells. Statistical significance is indicated as follows: * < $p = 0.05$, ** < $p = 0.01$, *** < $p = 0.001$.

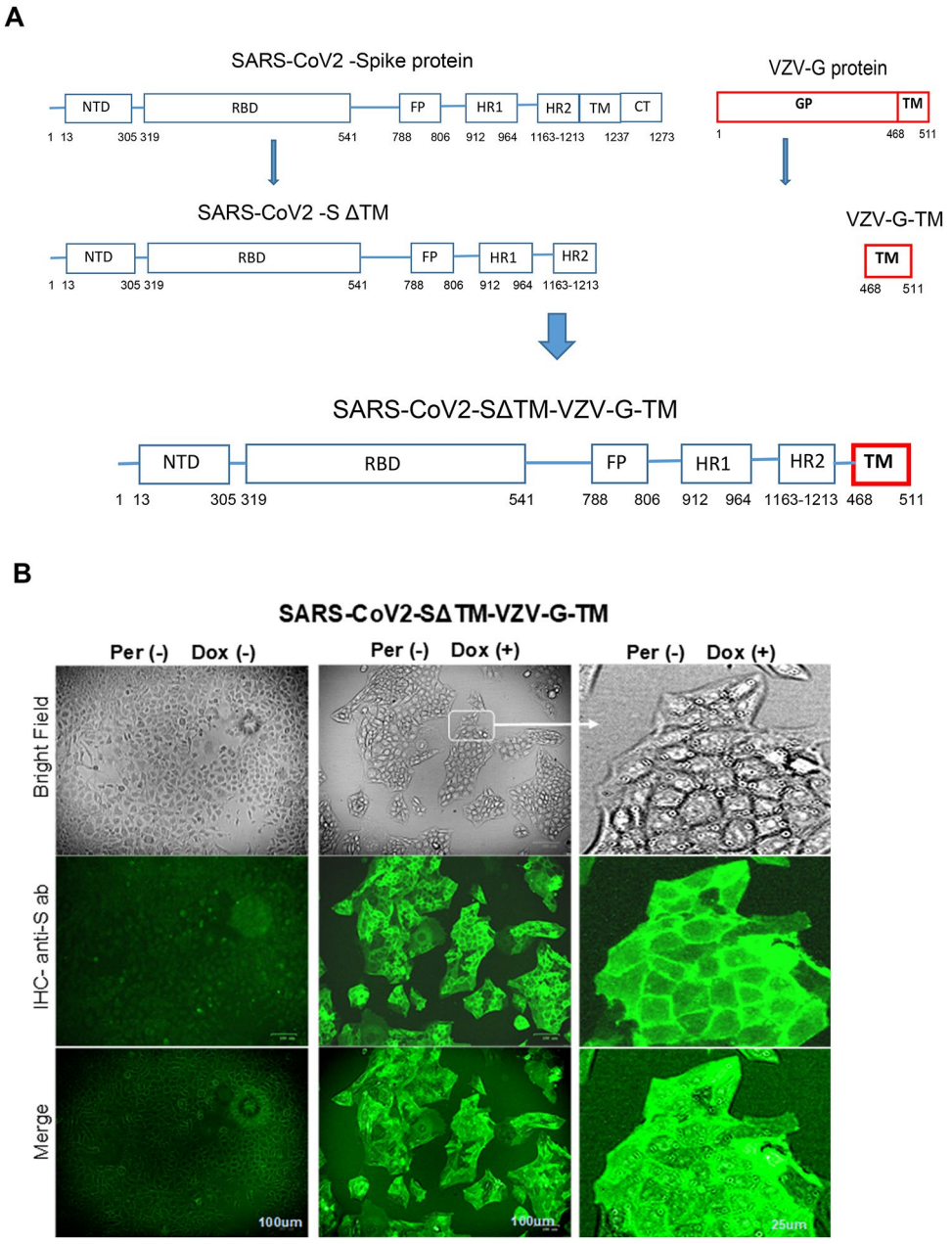

Fig. 8. Preparation of the SARS-CoV-2-SΔTM-VSV-G-TM construct and localization of the SARS-CoV-2 Spike protein in Renca cells. (**A**) Schematic representation of the content and preparation steps for the SARS-CoV-2-SΔTM-VSV-G-TM construct, in which the transmembrane domain of the SARS-CoV-2 Spike protein is replaced with that of the VSV-G protein. (**B**) Immunohistochemical (IHC) staining demonstrating the localization of the entire Spike protein to the Renca cell membrane in cells expressing SARS-CoV-2-SΔTM-VSV-G-TM, with staining performed without permeabilization. (**C**) IHC staining showing that the Spike protein in cells expressing SARS-CoV-2-SΔTM is localized to the cytoplasm, with IHC tests performed following permeabilization. (**D**) ELISA results investigating the presence of the SARS-CoV-2 Spike protein in cells expressing SARS-CoV-2-SΔTM-VSV-G-TM, SARS-CoV-2-SΔTM, and SARS-CoV-2-S Δ21. (**E**) IHC analysis of SPTA1 presence in cell membranes of cells expressing and not expressing SARS-CoV-2-SΔTM-VSV-G-TM, conducted without permeabilization. Grayscale representation was applied to visualize differences in IHC staining. Per (+) indicates the application of the permeabilization process, and Dox (+) indicates the addition of doxycycline.

Transfection Kit (631312-Takara Bio). After 48 h, supernatants containing rtTA virus were collected, and target cells were infected in the presence of 10 µg/ml polybrene (TR-1001, Sigma-Aldrich). After 24 h, the media of the cells was replaced with media containing 0.2-1 mg/ml neomycin (G418-RO, Sigma-Aldrich) and left for 10 to 15 days for selection. The surviving cells were pooled and named TA-Hep3B, TA-Renca, and TA-MAD109.

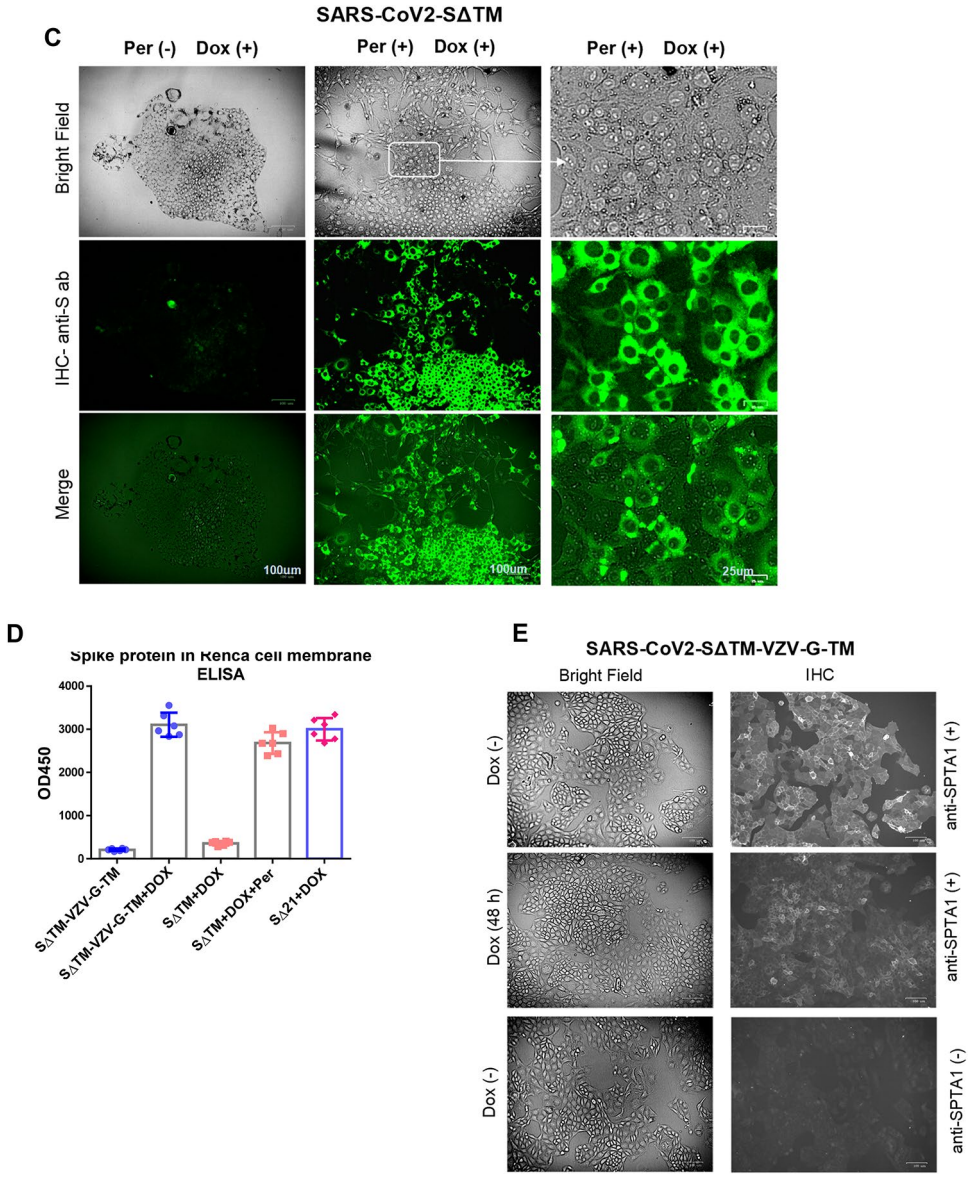

Figure 8. (continued)

Cloning of codon optimized for human SARS-CoV-2-S Wt and Δ21 (hSARS-CoV-2-S Wt and Δ21) and codon optimized for mouse SARS-CoV-2-S Wt and -S Δ21 (mSARS-CoV-2-S Wt and -S Δ21) genes into modified pBSK (pBSK-clo2D) subcloning vector plasmids

The hSARS-CoV-2-S wt, hSARS-CoV-2-S Δ21, mSARS-CoV-2-S wt, and mSARS-CoV-2-S Δ21 genes were inserted into the pBSK-clo2D vector construct, which was previously prepared with cloning sites in the pBSK (-) vector, including KpnI, ApaI, XhoI, SalI, PmeI, BamHI, EcoRV, EcoRI, XbaI, NotI, HindIII, MfeI, EcoRI, PstI, SmaI, BamHI, XbaI, BstXI, and SacI, to facilitate general DNA cloning in our laboratory. Blunt-ended SARS-CoV-2-S genes were inserted into the pBSK-clo2D plasmid cut with EcoRV and dephosphorylated using FastAP Thermosensitive Alkaline Phosphatase (Thermo Scientific-Thermo Fisher USA). The pBSK-hSARS-CoV-2-S wt, pBSK-hSARS-CoV-2-S Δ21, pBSK-mSARS-CoV-2-S wt, and pBSK-mSARS-CoV-2-S Δ21 vectors were obtained.

Cloning of codon optimized for human hSARS-CoV-2-S Wt and Δ21, and for mouse mSARS-CoV-2-S Wt and Δ21 genes into pRetroX-Tight-Pur vector

hSARS-CoV-2-S wt and S Δ21, and mSARS-CoV-2-S wt and S Δ21 genes were obtained from the pBSK-hSARS-CoV-2-S wt, pBSK-hSARS-CoV-2-S Δ21, and pBSK-mSARS-CoV-2-S wt and pBSK-mSARS-CoV-2-S Δ21 vectors, respectively, by cutting with the BamHI enzyme. The pRetroX-Tight-Pur vector was cut by BamHI restriction enzyme, dephosphorylated, and ligated with hSARS-CoV-2-S wt and S Δ21, and mSARS-CoV-2-S wt and S Δ21 cDNAs with compatible cohesive ends. After the orientation of the construct was determined, pRetroX-Tight-Pur-hSARS-CoV-2-S wt, pRetroX-Tight-Pur-hSARS-CoV-2-S Δ21, and pRetroX-Tight-Pur-

mSARS-CoV-2-S wt and pRetroX-Tight-Pur-mSARS-CoV-2-S Δ21 vectors were reproduced in large volumes using DH5α E. coli.

In the next step, HEK293T cells were transfected with the pRetroX-Tight-Pur-hSARS-CoV-2-S wt, pRetroX-Tight-Pur-hSARS-CoV-2-S Δ21, and pRetroX-Tight-Pur-mSARS-CoV-2-S wt and pRetroX-Tight-Pur-mSARS-CoV-2-S Δ21 vectors and helper vectors pCMV-VSV-G, pUMVC separately. After 48 h, supernatants of pRetroX-Tight-Pur-hSARS-CoV-2-S wt, pRetroX-Tight-Pur-hSARS-CoV-2-S Δ21, and pRetroX-Tight-Pur-mSARS-CoV-2-S wt and pRetroX-Tight-Pur-mSARS-CoV-2-S Δ21 vectors containing viruses with medium from the individual cells were collected, and rtTA expressing TA-Hep3B, TA-Renca, and TA-MAD109 target cells were infected. The infected clones were selected with 0.5-3 mg/ml puromycin (P9620-Sigma-Aldrich) for 6 days. Infected clones were maintained in the presence of 250 ng/ml puromycin. The expression of SARS-CoV-2-S wt and SARS-CoV-2-S Δ21 in individual cell lines was followed by dot blot and immunohistochemistry (IHC).

SARS-CoV-2-S ΔTM-VSV-G-TM, and SARS-CoV-2-S ΔTM cDNA preparation

The DNA sequence containing 1-1263 aa SARS-CoV-2-S ΔTM was obtained by PCR method, using the mouse mSARS-CoV-2 S Δ21 gene as a template, without a stop codon, and within the codon frame. The DNA sequence containing 468–511 aa SARS-CoV-2-S ΔTM was obtained by PCR method, using the mouse pCMV-VSV-G gene plasmid as a template, and within the codon frame. The two DNAs were then ligated and cloned into the pRetroX-Tight-Pur expression vector as described above. The DNA sequence containing 1-1263 aa SARS-CoV-2-S ΔTM was obtained by PCR method, using the mouse mSARS-CoV-2 S Δ21 gene as a template, with the stop codon at the C-terminal site, and within the codon frame.

Isolation of cell membrane

The membrane was isolated from cells as previously described with some modifications[22,23]. In brief, cells were harvested and resuspended at a concentration of 2.5×10^7 cells/mL in ice-cold Tris-magnesium buffer (TM buffer, pH 7.4, 0.01 M Tris and 0.001 M $MgCl_2$) and homogenized with a Dounce homogenizer to disrupt the cells. The cell homogenate was mixed with 1 M sucrose to a final concentration of 0.25 M sucrose, and then centrifuged at 2000 g and 4 °C for 10 min. The supernatant was collected and further centrifuged at 3000 g and 4 °C for 30 min to collect the cell membrane. The cell membrane was washed with ice-cold TM buffer with 0.25 M of sucrose and collected by centrifugation at 3000 g and 4 °C for 30 min.

Dot blot

Cell membrane-containing solution (also cytoplasmic extract) was diluted with PBS (137 mmol/L NaCl, 2.7 mmol/L KCl, 10 mmol/L Na2HPO4, and 1.8 mmol/L KH2PO4, pH 7.4) to 1×10^3 cells in 5 µL and applied onto a nitrocellulose membrane (NM). Then the dots were allowed to dry. The NM was completely immersed in blocking solution (5% non-fat skim milk in PBS) and then incubated for 60 min. The NM was immersed in a 1/100 dilution of antibodies or serum containing anti-SARS-CoV-2 S antibody in PBS-milk (5% non-fat skim milk in PBS) and incubated for one hour. The NM was washed three times with PBS-Tween. Depending on the primary antibody used (CALR, Calnexin, and GAPDH - Santa Cruz, USA; SPTA1, CDH2 - Solarbio, China), the NM was completely immersed with anti-human, anti-mouse, or anti-rabbit IgG antibody (Ab) conjugated with horseradish peroxidase (BioLegend, USA) diluted 1/1500 in PBS-milk, and incubated for 45 min. It was washed three times again with PBS-Tween. Finally, the blot reaction was revealed by immersing the membrane completely in the HRP chemiluminescence for 5 min and visualized by the Bio-Rad ChemiDoc system. Each NM was analyzed in duplicate. The intensity of dots was investigated using the ImageJ program (https://imagej.nih.gov/ij).

Whole cell ELISA preparation

The wells of 96-well cell culture plates were seeded with 1×10^3 TA-Hep3B, TA-Renca, and TA-MAD109 cells containing pRetroX-Tight-Pur-hSARS-CoV-2-S wt, pRetroX-Tight-Pur-hSARS-CoV-2-S Δ21, and pRetroX-Tight-Pur-mSARS-CoV-2-S wt and pRetroX-Tight-Pur-mSARS-CoV-2-S Δ21. Doxycycline (dox) was added after 24 h, and cells were fixed with 4% paraformaldehyde after 36 h.

ELISA Preparation with S1 of SARS-CoV-2 S

ELISA plates were coated overnight with 20 ng/mL of SARS-CoV-2 S1-RBD (BioLegend, USA), diluted in a coating buffer, and applied to all 96 wells of the plates.

Antibody measurements using whole cell or cell membrane coated ELISA

The total levels of IgG and anti-SARS-CoV-2-S antibodies in individuals who have been infected or vaccinated were measured by the prepared ELISAs described above. Ninety-six-well cell culture plates with cells containing hSARS-CoV-2-S wt, hSARS-CoV-2-S Δ21, mSARS-CoV-2-S wt, and mSARS-CoV-2-S Δ21 proteins on the cell membrane, or coated with the cell membrane containing SARS-CoV-2-S protein, were blocked with 5% milk in PBS for 1.5 h at room temperature (RT). Serum samples from each immunization group were diluted in PBS-Tween-1% milk, added to plates, and incubated for 1 h at RT. Plates were then washed, and secondary HRP-conjugated anti-human IgG antibodies (BioLegend; all diluted 1:1,000 in PBS-Tween-1% milk) were added and incubated for 45 min at RT. Plates were washed again, and the o-phenylenediamine dihydrochloride (OPD) substrate (Sigma-Aldrich; 0.5-1.0 mg/mL OPD was dissolved in buffer—0.05 M citric acid, 0.05 M sodium phosphate; pH 5) with 1 µL 30% hydrogen peroxide per 1 mL of substrate was added. The reaction was stopped by adding 1 M H2SO4. Absorbance was read at 450 nm.

Expression analysis of SARS-CoV-2-S by immunofluorescence microscopy

Immunofluorescence experiments were performed on SARS-CoV-2-S Δ21 expressing Hep3B, Renca, and MAD109 cells. Twenty-four hours after splitting the cells, dox was added to all cells except for the control group. The cells were incubated with serum positive for SARS-CoV-2-S from a patient infected with SARS-CoV-2 or an anti-S antibody (BioLegend) after fixation with buffered formalin (4%) solution at 12, 24, and 48 h post-dox addition. Anti-SARS-CoV-2-S was detected with rabbit or human secondary antibodies conjugated with the FITC fluorochrome (BioLegend; diluted 1:1000). Hoechst (Sigma) was used to stain the cell nuclei. Images of sections of the cells were taken with a fluorescence microscope.

Ethics statement

Mice studies were carried out at Ankara University Medical School Experimental Animal Care Unit under permission of the Local Ethics Committee for Animal Experiments at Ankara University with the supervision of a veterinarian (File No: 2021-54; permit number: 2021 – 1074). The animal protocols were approved by the Local Ethics Committee for Animal Experiments at Ankara University (A.U.). All animal experiments and methods were performed in accordance with the animal experimentation guidelines and regulations approved by the Local Ethics Committee for Animal Experiments at A.U. Following observation of the mice's condition for at least six months after the second dose of vaccination, the mice were euthanized using carbon dioxide asphyxiation in their own cages. The study was carried out in compliance with the ARRIVE guidelines. Live virus studies were completed in the General Directorate of Public Health, Microbiology Reference Laboratory (Animal Biosafety Level 3 plus - ABSL3+) in Ankara, Turkey.

Animal immunization

The Balb/c and C57BL/6 mouse groups used in the experiments were obtained from the A.U. Medical School Experimental Animal Care Unit. This unit is controlled, supervised, and operates under the permission of the Local Ethics Committee for Animal Experiments at Ankara University. Balb/c and C57BL/6 mouse groups (4 animals per group) were immunized subcutaneously with 5×10^4 whole cells expressing TA-Renca-mSARS-CoV-2-S in a volume of 100 µL after being killed by UV, or with cell membrane obtained from 5×10^4 TA-Renca-mSARS-CoV-2-S Δ21 expressing cells in a volume of 100 µL at the A.U. Medical School Experimental Animal Care Unit. The cells and cell membranes were obtained 36 h after the addition of dox to the growing cell culture. The cell membrane was isolated according to the protocol described above, and the cells were collected by scraping and washing three times with PBS. These were administered to mice with complete Freund's adjuvant (CFA, Sigma-Aldrich) on the 1st and 15th days. In the second vaccination, incomplete Freund's adjuvant was used. IgG titers were determined by ELISA in sera collected on day 15 or 28 post-vaccination from mice immunized with cells or cell membranes containing mSARS-CoV-2-S Δ21. The control group received PBS with CFA or the same amount of cell membrane from Renca wt cells. Furthermore, 3 animals per group were immunized with 1×10^4 TA-Renca-mSARS-CoV-2-S Δ21 cells or cell membranes obtained from the 1×10^4 TA-Renca-mSARS-CoV-2-S Δ21 cell line without CFA, and 4 animals per group were immunized with PBS + CFA as a placebo. At the same time periods, 4 mice were immunized with the Pfizer-BioNTech Covid-19 mRNA S vaccine (BNT162b2) administered at the dose of mL/kg described for adult humans (after dilution of BNT162b2, 0.3 mL for each adult), and another 4 groups of mice were immunized with the inactivated whole virus vaccine (Sinovac-Coronavac Covid-19) (WIV) administered at the dose of mL/kg described for adult humans (0.5 mL for each adult). Blood samples were collected from the tail vein on days 15 and/or 28 and were used to measure antibody titer and perform virus neutralization assays.

Furthermore, 3 animals per group were immunized with 1×10^6 live TA-Renca-mSARS-CoV-2-S Δ21 cells or the 1×10^6 live TA-Renca-mSARS-CoV-2-S wt cell line. On the same day, doxycycline was added to the drinking water of the animals. In addition, after treatment with dox for 24 h in vitro, live Hep3B cells containing pRetroX-Tight-Pur-hSARS-CoV-2-S wt or pRetroX-Tight-Pur-hSARS-CoV-2-S Δ21 were administered subcutaneously in mice. Blood samples were collected on day 14 until tumor formation was observed (usually for 10–15 days for Renca cells), and SARS-CoV-2-S specific IgM, IgA, and IgG were analyzed. Blood from each individual mouse was collected and processed to obtain serum samples to analyze the titers of IgG antibodies, IgG isotypes, and neutralizing antibodies against SARS-CoV-2. Body weight, food, and water consumption of vaccinated mice were measured for 4 months, and clinical observations such as changes in skin, fur, eyes, mucous membranes, occurrence of secretions or excretions, changes in gait and posture, the presence of clonic or tonic movements, stereotypes, or bizarre behavior were monitored.

Immunogenicity evaluation of vaccinations

To detect antibody levels in the sera of mice vaccinated with cells or cell membranes containing mSARS-CoV-2-S Δ21, geometric dilutions of the sera were used for the immunogenicity analyses by ELISA. The endpoint titer was defined as the reciprocal serum dilution that produced a mean OD value at least two times greater than that of the pre-immune control samples.

Enzyme-linked immunosorbent assay (ELISA)

The total levels of IgG and anti-SARS-CoV-2-S antibodies in individual immunized mice were measured by ELISA. Ninety-six-well cell culture plates with cells containing mSARS-CoV-2-S were blocked with 5% milk in PBS for 2 h at room temperature (RT). To detect antibody levels in the sera of mice vaccinated with cells or cell membranes containing mSARS-CoV-2-S Δ21, twofold serial dilutions of the sera were used for the immunogenicity analyses. Serum samples from each immunization group were diluted in PBS-Tween with 1% milk, added to plates, and incubated for 1 h at RT. Plates were then washed, and secondary HRP-conjugated anti-mouse IgG antibodies (BioLegend; all diluted 1:1000 in PBS-Tween-1% milk) were added and incubated for

45 min at RT. Plates were washed, the OPD substrate (Sigma-Aldrich) was added, and the reaction was stopped by adding 1 M H2SO4. Absorbance was read at 450 nm. Total IgG titers were measured as the highest dilution that produced an absorbance at 450 nm at least two times higher than the absorbance of naive serum.

TA-Renca-mSARS-CoV-2-S whole cell neutralization assay

To compare the neutralizing effects of different vaccines, we used a method we developed for this purpose (Renca-S cell Neutralization Assay). Briefly, whole cells obtained from the 1×10^6 TA-Renca-mSARS-CoV-2-S Δ21 cells after 36 h of dox induction (total 1 mL PBS) were used for the neutralization assay after three washes with PBS (Fig. 4A). 100 µL of TA-Renca-mSARS-CoV-2-S Δ21 cells were incubated with two-fold serially diluted mouse sera for 1 h at 37 °C. The mixtures were then centrifuged, and the supernatant was used in the ELISA with S1 protein (BioLegend) coated 96-well plates. Relative endpoint neutralization titers were determined. The neutralization endpoint was defined as the highest dilution that produced an absorbance at 450 nm at least two times higher than the absorbance of naive serum.

Live SARS-CoV-2 neutralization assay

The presence of virus-specific neutralizing antibodies in mice vaccinated with CM-S, mRNA-S, and WIV was evaluated via a virus neutralization assay. Serially diluted serum samples (two-fold in DMEM) were mixed with an equal volume of virus at a 100 TCID50 titer (1:1000) in duplicate and incubated for 1 h at 37 °C. The serum-virus mixtures were then inoculated onto one-day-old, 90% confluent Vero E6 cells grown in 96-well plates. The infected cells were further incubated under identical conditions for four days. The test was evaluated using an inverted microscope when 100% CPE was observed in virus control wells. Neutralization titers were defined as the serum dilution required for 50% neutralization of viral infection. Live virus studies were completed in the General Directorate of Public Health, Microbiology Reference Laboratory (Animal Biosafety Level 3 plus - ABSL3+) in Ankara, Turkey.

Splenocytes isolation

Spleens were aseptically collected from mice and separated using Pluri Bead-pluristrainer 70 µm (pluri-Select USA), then stored in 1× PBS on ice. Splenocytes were isolated, and red blood cells (RBCs) were lysed using a hypotonic solution with RBD blood lysis buffer (BioVision). Cytokines in the supernatant of mouse splenocytes (1×10^6 cells/mL) were analyzed after 12 h of incubation with 50 ng of S1 protein (Recombinant SARS-CoV-2 S Protein S1 [carrier-free], BioLegend).

Flow cytometric analysis

The LEGENDplex Mouse Inflammation Panel (13-plex) (BioLegend) was used to study cytokine responses. The manufacturer's setup instructions were followed for flow cytometric analysis (www.biolegend.com/legendplex).

Statistical analysis

All data are expressed as means ± standard errors of the means. For all analyses, P values were obtained using Student's t-test (unpaired, two-tailed) or Spearman rank-correlation tests. All graphs were generated using Microsoft Excel or GraphPad Prism v6.0. The data are based on results from at least three independent experiments. Error bars represent standard deviations.

Data availability

The data generated in the present study may be requested from the corresponding author.

Received: 21 January 2025; Accepted: 21 March 2025
Published online: 29 March 2025

References

1. Edgar, J. R. Q&A: what are exosomes, exactly? *BMC Biol.* **14**, 46. https://doi.org/10.1186/s12915-016-0268-z (2016).
2. Xie, F., Huang, Y., Zhan, Y. & Bao, L. Exosomes as drug delivery system in Gastrointestinal cancer. *Front. Oncol.* **12**, 1101823. https://doi.org/10.3389/fonc.2022.1101823 (2023).
3. Li, J. et al. Macrophage Membrane-Coated Nano-Gemcitabine promotes lymphocyte infiltration and synergizes AntiPD-L1 to restore the tumoricidal function. *ACS Nano Jan.* **10** (1), 322–336. https://doi.org/10.1021/acsnano.2c07861 (2023).
4. Du, J. et al. Preparation of C6 cell membrane-coated doxorubicin conjugated manganese dioxide nanoparticles and its targeted therapy application in glioma. *Eur. J. Pharm. Sci.* **180**, 106338. https://doi.org/10.1016/j.ejps.2022.106338 (2023).
5. Huang, Y., Yang, C., Xu, X., Xu, W. & Liu, S. Structural and functional properties of SARS-CoV-2 Spike protein: potential antivirus drug development for COVID-19. *Acta Pharmacol. Sin.* **41**, 1141–1149. https://doi.org/10.1038/s41401-020-0485-4 (2020).
6. Vennema, H., Heijnen, L., Zijderveld, A., Horzinek, M. C. & Spaan, W. J. Intracellular transport of Recombinant coronavirus Spike proteins: implications for virus assembly. *J. Virol.* **64**, 339–346. https://doi.org/10.1128/JVI.64.1.339-346.1990 (1990).
7. Lontok, E., Corse, E. & Machamer, C. E. Intracellular targeting signals contribute to localization of coronavirus Spike proteins near the virus assembly site. *J. Virol.* **78**, 5913–5922. https://doi.org/10.1128/JVI.78.11.5913-5922.2004 (2004).
8. Boson, B. et al. The SARS-CoV-2 envelope and membrane proteins modulate maturation and retention of the Spike protein, allowing assembly of virus-like particles. *J. Biol. Chem.* **296**, 100111. https://doi.org/10.1074/jbc.RA120.016175 (2021).
9. Khan, W. H. et al. COVID-19 pandemic and vaccines update on challenges and resolutions. *Front. Cell. Infect. Microbiol.* **11**, 690621. https://doi.org/10.3389/fcimb.2021.690621 (2021).
10. Lazebnik, Y. Cell fusion as a link between the SARS-CoV-2 spike protein, COVID-19 complications, and vaccine side effects. Dec 7;12(25):2476–2488. (2021). https://doi.org/10.18632/oncotarget.28088
11. Firacative, C. et al. Identification of T helper (Th)1- and Th2-associated antigens of Cryptococcus neoformans in a murine model of pulmonary infection. *Sci. Rep.* **8** (1), 2681. https://doi.org/10.1038/s41598-018-21039-z (2018).
12. Mountford, A. P., Fisher, A., Wilson, R. A. & R.A The profile of IgG1 and IgG2a antibody responses in mice exposed to schistosoma mansoni. *Parasite Immunol.* **16**, 10521–10527. https://doi.org/10.1111/j.1365-3024,.1994.tb00306.x (1994).

13. Tahtinen, S. et al. IL-1 and IL-1ra are key regulators of the inflammatory response to RNA vaccines. *Nat. Immunol.* 23, 532–542, https://doi.org/10.1038/s41590-022-01160-y(2022).
14. Netea, M. G. et al. Defining trained immunity and its role in health and disease. *Nat. Rev. Immunol.* **20** (6), 375–388. https://doi.org/10.1038/s41577-020-0285-6 (2020).
15. Raeber, M. E., Zurbuchen, Y., Impellizzieri, D. & Boyman, O. The role of cytokines in T-cell memory in health and disease. *Immunol. Rev.* **283** (1), 176–193. https://doi.org/10.1111/imr.12644 (2018).
16. Guttormsen, H. K., Wetzler, L. M., Finberg, R. W. & Kasper, D. L. Immunologic memory induced by a glycoconjugate vaccine in a murine adoptive lymphocyte transfer model. *Infect. Immun.* **66** (5), 2026–2032. https://doi.org/10.1128/IAI.66.5.2026-2032.1998 (1998).
17. Nicolini, A., Ferrari, P. & Biava, P. M. Exosomes and cell communication: from tumour-Derived exosomes and their role in tumour progression. *Cancers (Basel)*. **13** (4), 822. https://doi.org/10.3390/cancers13040822 (2021).
18. Neller, M. A., Lópeza, J. A. & Schmidt, C. W. Antigens for cancer immunotherapy. *Semin. Immunol.* **20**, 286–295. https://doi.org/10.1016/j.smim.2008.09.006 (2008).
19. Rhea, E. M. et al. The S1 protein of SARS-CoV-2 crosses the blood-brain barrier in mice. *Nat. Neurosci.* **24** (3), 368–378. https://doi.org/10.1038/s41593-020-00771-8 (2021).
20. Suzuki, Y. J. et al. SARS-CoV-2 Spike protein-mediated cell signaling in lung vascular cells. *Vascul Pharmacol.* **137**, 106823. https://doi.org/10.1016/j.vph.2020.106823 (2021). Epub 2020 Nov 21.
21. Rodrigues Prestes, T. R., Rocha, N. P., Miranda, A. S., Teixeira, A. L. & Simoes-E-Silva, A. C. The Anti-Inflammatory potential of ACE2/Angiotensin-(1–7)/Mas receptor axis: evidence from basic and clinical research. *Curr. Drug Targets*. **18** (11), 1301–1313. https://doi.org/10.2174/1389450117666160727142401 (2017).
22. Zhai, Y. et al. Preparation and application of cell Membrane-Camouflaged nanoparticles for cancer therapy. *Theranostics* **7** (10), 2575–2592. https://doi.org/10.7150/thno.20118 (2017). eCollection 2017.
23. Cao, H. et al. Liposomes coated with isolated macrophage membrane can target lung metastasis of breast cancer. *ACS Nano*. **10** (8), 7738–7748. https://doi.org/10.1021/acsnano.6b03148 (2016).

Acknowledgements

We would like to thank Nazli Aydin and Veterinarian Dr. Atilla İşgören for the care of the animals and the experiments performed. We would like thank Editage's English Editing services for their invaluable assistance. We would like thank Dr. Irem Kar for assistance in Statistics.

Author contributions

Conceptualization and designing the experiments: FS. Performing the Investigations: FS, BTA, SY, VCB. Research expenses: FS. Project administration: FS. Supervision: FS. Writing – original draft: FS. All authors reviewed the manuscript.

Funding

This study did not receive any specific funding. All expenses were personally covered by FS.

Declarations

Ethics approval and consent to participate

Mice studies were carried out at Ankara University Medical School Experimental Animal Care Unit under permission of the Local Ethics Committee for Animal Experiments at Ankara University with the supervision of a veterinarian ((File No:2021-54; permit number:2021 – 1074). The animal protocols were approved by the Local Ethics Committee for Animal Experiments at Ankara University (A.U.). All animal experiments and methods were performed in accordance with the animal experimentation guidelines and regulations approved by the Local Ethics Committee for Animal Experiments at A.U. Following observation of the mice's condition for at least six months after the second dose of vaccination, the mice were euthanized using carbon dioxide asphyxiation in their own cages. The study was carried out in compliance with the ARRIVE guidelines. Live virus studies were completed in the Generel Directorate of Public Health, Microbiology Reference Laboratory (Animal Biosafety Level 3 plus - ABSL3þ) in Ankara-Turkey.

Competing interests

The authors declare no competing interests.

Additional information

Supplementary Information The online version contains supplementary material available at https://doi.org/10.1038/s41598-025-95503-y.

Correspondence and requests for materials should be addressed to F.S.

Reprints and permissions information is available at www.nature.com/reprints.

Publisher's note Springer Nature remains neutral with regard to jurisdictional claims in published maps and institutional affiliations.